DEPARTMENT OF CHEMISTRY
University of Cape Town

DIPARTIMENTO DI SCIENZE CHIMICHE, DELLA VITA
E DELLA SOSTENIBILITÀ AMBIENTALE
Università di Parma

DISSERTATION PRESENTED FOR THE DEGREE OF MASTER OF SCIENCE IN

CHEMISTRY

University of Cape Town

Synthesis and Optimization of Ergothioneine Derivatives

Supervisors:
Professor Anwar Jardine
Professoressa Laura Baldini

By:
Anita Ballerini

July 2025

The copyright of this thesis vests in the author. No quotation from it or information derived from it is to be published without full acknowledgement of the source. The thesis is to be used for private study or non-commercial research purposes only.

Published by the University of Cape Town (UCT) in terms of the non-exclusive license granted to UCT by the author.

University of Cape Town

Acknowledgements

First and foremost, I would like to sincerely thank my supervisor, Professor Anwar Jardine, for his constant availability and guidance throughout my stay in Cape Town. Thank you for making this experience possible, an experience that has been the most meaningful and enriching of my life, and for welcoming us so warmly, making us feel at home from the very beginning in the wonderful city you live in.

I am also deeply grateful to the entire research group led by Professor Jardine. A special thanks to Maryam Fredericks, my "lab mom", for her patience and support, and to Nabanita Chatterjee for her kindness and help throughout the project. I would also like to thank Mymoena, Sitara, and Malikah for their support and companionship in the lab.

My heartfelt thanks go to all the friends and fellow adventurers I met at the P.D. Hahn building, who made us feel at home from day one: Shan, Leah, Nicole, Joseph, Jarid, Larnelle and CJ, Lebo, Melissa, Gciniwe, Fatima, and Farhaan.

To Professor Luigi Nassimbeni, thank you for your charisma, your chocolates, and your stories, you made us feel at home uniquely and unforgettably.

A warm thank you to Joanne Polzin for always being there when we needed support and for helping us navigate through all the administrative and bureaucratic matters with kindness and efficiency.

And finally, thank you to Eri and Guli for becoming my family during the six unforgettable months spent in Cape Town.

Table of Contents

Abstract

Ergothioneine (EGT, **Figure a**) is a naturally occurring sulfur-containing amino acid derived from histidine, known for its antioxidant properties in living organisms and its significant potential in the pharmaceutical and cosmetic industry.

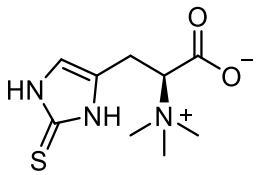

Figure a. *Chemical structure of ergothioneine.*

The objective of this study is to establish an effective protocol for the synthesis and purification of EGT derivatives that could lead to high purity sustainably produced product. A key challenge was balancing reaction efficiency with selective thiolation which required a systematic refinement of experimental conditions free from chromatography.

Purification strategies were adjusted throughout the project to achieve maximal purity. Since column chromatography have proven to be limiting due to the high polarity of the target compound, solid-liquid and liquid-liquid extractions were employed as alternative methods. These methodologies not only enabled the efficient separation of the target compound from related impurities but were also more appropriate for large-scale applications.

Furthermore, the antioxidant capacity of L-(+)-ergothioneine was compared with cysteine using the ABTS decolorization assay. The ABTS assay is a widely employed method for quantifying radical scavenging activity relative to Trolox, a vitamin E analogue, used as the standard antioxidant.

We found that L-(+)-ergothioneine is efficient at scavenging $ABTS^{\bullet+}$ radical cations, similar to that of Trolox and cysteine. These results provide important information about the free radical scavenging activities of these derivatives and their potential nutraceutical, pharmaceutical and biomedical applications.

Abbreviation list

ABTS	2,2'-Azino-bis(3-ethylbenzothiazoline-6-sulfonicacid)diammonium salt
ACN	Acetonitrile
NH_4Cl	Ammonium chloride
δ	Chemical shift
d (NMR)	Doublet
dd (NMR)	Doublet of doublets
H-D-Pen-OH	D-penicillamine
HOBr	Hypobromous acid
EgtA	γ-glutamylcysteine ligase
EgtB	Hercynine oxygenase
EgtC	γ-glutamyl-hercynylcysteine sulfoxide hydrolase
EgtD	Histidine *N*-α-methyltransferase
EgtE	Hercynylcysteine S-oxide lyase
EGT	L-(+)-ergothioneine
EtOH	Ethanol
EtOAc	Ethyl acetate
HPLC	High-performance liquid chromatography
HRMS	High-resolution mass spectrometry
HCl	Hydrochloric acid
LCMS	Liquid chromatography mass spectrometry
LMW	Low molecular weight
NBS	*N*-bromosuccinimide
NMR	Nuclear magnetic resonance

OCTN1	Organic cation transporter
OvoA	Iron(II) dependant sulfoxide synthase
Ppm	Parts per million
ROS	Reactive oxygen species
Rt	Room temperature
SET	Single Electron Transfer
s (NMR)	Singlet
TIC	Total Ion Current
TFA	Trifluoroacetic acid
t (NMR)	Triplet
TEAC	Trolox Equivalent Antioxidant Capacity
TE	Trolox Equivalents
2D-NMR	Two-dimensional nuclear magnetic
UPLC-MS/MS	Ultra-performance liquid chromatography-tandem mass spectrometry
UV-Vis	Ultra-violet visible
VCS	Validating claim support

General Introduction

Low-molecular-weight (LMW) thiols are small sulfur-containing compounds that play a crucial role in maintaining cellular redox balance and protecting biomolecules from oxidative damage. Glutathione (GSH) is the most widely distributed intracellular antioxidant. Ergothioneine (EGT), another low-molecular-weight thiol, is a powerful natural antioxidant that has recently attracted scientific interest due to its unique chemical properties and potential therapeutic applications. This compound is synthesised by certain fungi, bacteria, and cyanobacteria but is not produced by humans or animals, so we must obtain it via dietary intake.

Key Features of Ergothioneine

EGT was first isolated by Tanret in 1909 from ergot (*Claviceps purpurea*), the fungal infection of rye grain.[1] EGT was later identified as a sulfur-containing thiourea derivative of the amino acid histidine and exists in an equilibrium between two forms: the thiol and thione forms (**Figure 1.1**). When EGT is absorbed by the organic cation transporter (OCTN1), it is not rapidly metabolised, unlike other antioxidants. EGT is therefore capable of accumulating to high levels in the body, and this allows EGT to retain its antioxidant activity under normal physiological conditions for extended periods.[2]

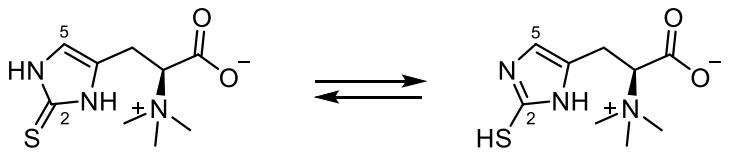

Figure 1.1. *Chemical structure of ergothioneine.*

The sulfhydryl group present in the EGT structure, occurring at the C2 atom of the imidazole ring, contributes to its broad biological effects, such as powerful antioxidant, anti-inflammatory, and detoxifying properties.[3]

EGT has numerous advantages compared to other known antioxidants due to its exceptional physiochemical stability, particularly in oxidative environments, and its selective accumulation in tissues prone to oxidative stress (such as the brain, liver, kidneys and eyes). Ergothioneine's accumulation in these organs suggests it plays a crucial role in protecting them against oxidative stress in critical areas of the body. Moreover, it is known to be non-toxic as it can build up in millimolar concentrations in some tissues in the body without causing toxicity.[4] In the brain, for example, ergothioneine may help in reducing neurodegenerative damage associated with conditions like Alzheimer's disease and Parkinson's disease. In the liver and kidneys, its protective properties suggest that it could help reduce liver fibrosis and kidney damage, which are often linked to excessive oxidative stress. Oxidative stress is caused by an imbalance between prooxidants and antioxidants, leading to damage at the biomolecular level, particularly to DNA, lipids, proteins, and carbohydrates. This imbalance results from an excess of prooxidants, such as free radicals like hydroxyl radical ($OH^{\bullet}$) and reactive oxygen species (ROS) like peroxynitrite ($ONOO^-$) and hypochlorous acid (HClO). These prooxidants intensify oxidative stress by accelerating the oxidation processes.[5] Biothiols like EGT exert their antioxidant effects by reacting with ROS. The thiol group (-SH), present in the structure, interacts with the ROS, neutralising them. In this process, the biothiol is oxidized, forms a disulfide and loses its reducing capacity.[6]

$$R - SH + \cdot OH \rightarrow R - S\cdot + H_2O \qquad (1)$$

$$2\,R - S\cdot \rightarrow R - S - S - R \qquad (2)$$

This transformation not only reduces the harmful effect of ROS but also protects critical cellular components, such as DNA, lipids, and proteins (which are often involved in the pathogenesis of age-related diseases and various pathological conditions) from oxidative damage.

Thiol-containing antioxidants have such a significant role in the body that low levels of them contribute to various illnesses, including liver failure, coronary artery disease and even strokes.[7]

Sources of Ergothioneine

Animals as well as humans do not synthesize EGT, and they acquire it from their diet. Foods rich in EGT include mushrooms, corn, oats and meat. It is, instead, naturally synthesised in organisms such as, *Mycobacteria, Cyanobacteria, Neurospora crassa,* as well as fungi and mushrooms.[8] Among these, edible fungi, particularly mushrooms, serve as the primary dietary source of EGT, accounting for approximately 95% of total dietary intake.[9] The concentration of EGT varies significantly across different mushroom species, likely due to variations in the availability and bioaccessibility of key precursors for its biosynthesis, such as histidine, cysteine, and methionine, which are present in varying amounts across species.[10] The European Food Safety Authority (EFSA) has confirmed that synthetic EGT can be safely consumed under recommended dosages of 30 mg/day for adults and 20 mg/day for children.[11]

In fungi such as *Neurospora crassa*, EGT is biosynthesized and subsequently incorporated into the food chain when plants or animals ingest these fungi. Once consumed, EGT is absorbed and concentrated into cells and tissues by a specific organic cation transporter OCTN1 (also known as ergothioneine transporter, ETT).[12] The expression of OCTN1 varies across different tissues, leading to significant variation in EGT accumulation.[8] OCTN1 operates within the intestinal tract, facilitating the absorption of EGT from dietary sources, and is then able to redistribute EGT to various cells and tissues through the bloodstream.

Beyond its well-documented presence in mushrooms, ergothioneine is found in a variety of other foods, including legumes, whole grains, and animal-derived products, each contributing to overall dietary intake and potential health benefits.

In addition to mushrooms, legumes such as kidney beans and black beans represent a significant dietary source of ergothioneine.[13,14]

These plant-based foods provide a significant contribution to EGT intake. While the concentrations of EGT in legumes are lower than those found in mushrooms, their widespread consumption makes them an important dietary source of this compound.

Whole grains, including oat bran and wheat germ[14], also contribute to ergothioneine consumption. These grains are considered moderate sources of EGT and offer additional nutritional benefits, such as dietary fibres, essential vitamins, and polyphenols, which promote metabolic and cardiovascular health.

Meat and organ tissues also contain detectable levels of this compound. The bioaccumulation of EGT in animal tissues occurs due to the ingestion of plants and fungi that contain high levels of ergothioneine.[15,4] The presence of EGT in animal tissues suggests its physiological significance in mammalian systems, as it is actively transported and retained via the OCTN1 transporter. Consequently, individuals who include animal products in their diet may obtain ergothioneine from meat sources.

Potential Health Benefits

As mentioned before, thanks to its antioxidant capacity, ergothioneine is considered to play a key function by taking part in many different physiological processes that can help protect our bodies from the harmful effects of oxidative stress, which is thought to be a major contributor to several chronic diseases.

The neuroprotective effects of ergothioneine are of significant interest, particularly in the context of neurodegenerative diseases such as Alzheimer's and Parkinson's.[8,16] Research has shown that ergothioneine, due to its ability to selectively accumulate in neural tissues, can neutralize reactive oxygen species (ROS) and reactive nitrogen species (RNS).[17]

By scavenging free radicals, ergothioneine helps to prevent oxidative damage to neurons, preserves mitochondrial function, and reduces the aggregation of misfolded proteins, which are characteristics of neurodegenerative diseases.

Besides its neuroprotective role, ergothioneine has been demonstrated to have positive effects on cardiovascular health. Oxidative stress is a significant factor in dysfunction of the endothelium, which can lead to such cardiovascular diseases as atherosclerosis, hypertension and others.[18] This is reduced by ergothioneine, which speeds up the repair of oxidative damage to endothelial cells and helps to maintain vascular health. Furthermore, ergothioneine's anti-inflammatory properties contribute to the reduction of inflammatory cytokine production, which is crucial in managing chronic inflammatory conditions associated with cardiovascular disease.[19]

Lastly, EGT has attracted attention for its potential in the field of ageing and prolonging life.[20] Oxidative stress is a well-established factor in aging and age-related diseases, including cardiovascular disease, cognitive decline, and metabolic disorders. Its antioxidant activity contributes to the maintenance of cellular functions in repair and survival, all necessary components if one wants to age healthily. Also, by preserving the integrity of mitochondria and reducing ROS-induced cellular damage, it seems that ergothioneine can extend lifespan and reduce the onset of age-associated diseases.

Ergothioneine in cosmetic products

Beyond its physiological importance, EGT is commonly used in cosmetic formulations, such as facial creams, due to its anti-aging properties, particularly its ability to reduce oxidative damage in the skin.[21] The skin, as the largest organ in the human body, is constantly exposed to external harmful factors like air pollution and ultraviolet (UV) radiation. Over time, this exposure can result in oxidative damage that accelerates skin aging and promotes inflammation.

The EGT transporter, OCTN1, is expressed by skin cells, with the highest levels found in the epidermis. Specifically, the basal and granular layers of the epidermis play a key role in skin repair, as they are involved in continuous cell division.[22]

Many cosmetic products are marketed with anti-aging claims, such as reducing wrinkles, minimizing pore size, and improving skin firmness and elasticity. However, these products must undergo rigorous clinical testing by organizations like Validating Claim Support (VCS) to verify their efficacy [23]. Among these products, those containing L-(+)-ergothioneine often promote themselves as anti-aging solutions that improve skin appearance. Therefore, it is essential to ensure that these products genuinely contain L-(+)-ergothioneine, as advertised.

Synthesis of Ergothioneine Derivatives

Introduction: Overview of Ergothioneine Synthetic Routes

Biosynthesis

The biosynthesis of L-(+)-ergothioneine in fungi and bacteria is carried out by the action of five enzymes, as shown in **Scheme 2.1**, encoded by the genes *EgtA, EgtB, EgtC, EgtD, and EgtE*.[24]

The process begins with EgtD, a SAM-dependent methyltransferase, which catalyses the methylation of histidine to produce hercynine, a trimethyl ammonium betaine. Hercynine is a central intermediate that undergoes sulfur incorporation in subsequent steps.

EgtA, a γ-glutamylcysteine ligase, facilitates the formation of γ-glutamylcysteine by catalysing the ATP-dependent conjugation of glutamate and cysteine. γ-glutamylcysteine serves as the sulfur donor for the next steps.

Hercynine is then transformed into *S*-(β-amino-β-carboxyethyl)ergothioneine sulfoxide (**II**) through the action of EgtB, an iron(II)-dependent oxidase. This enzyme requires oxygen and γ-glutamylcysteine to generate γ-glutamylcysteinyl hercynine (**I**). However, the precise mechanism of this transformation, particularly the sulfoxide formation, remains under investigation.

Next, EgtC, a putative class-II glutamine amidotransferase, catalyses the hydrolysis of the *N*-terminal glutamic acid, yielding *S*-(β-amino-β-carboxyethyl)ergothioneine sulfoxide (**II**).

Finally, the last step is carried out by the enzyme EgtE, a pyridoxal 5′-phosphate (PLP)-dependent β-lyase, which converts the intermediate into the final product, L-(+)-ergothioneine (EGT).

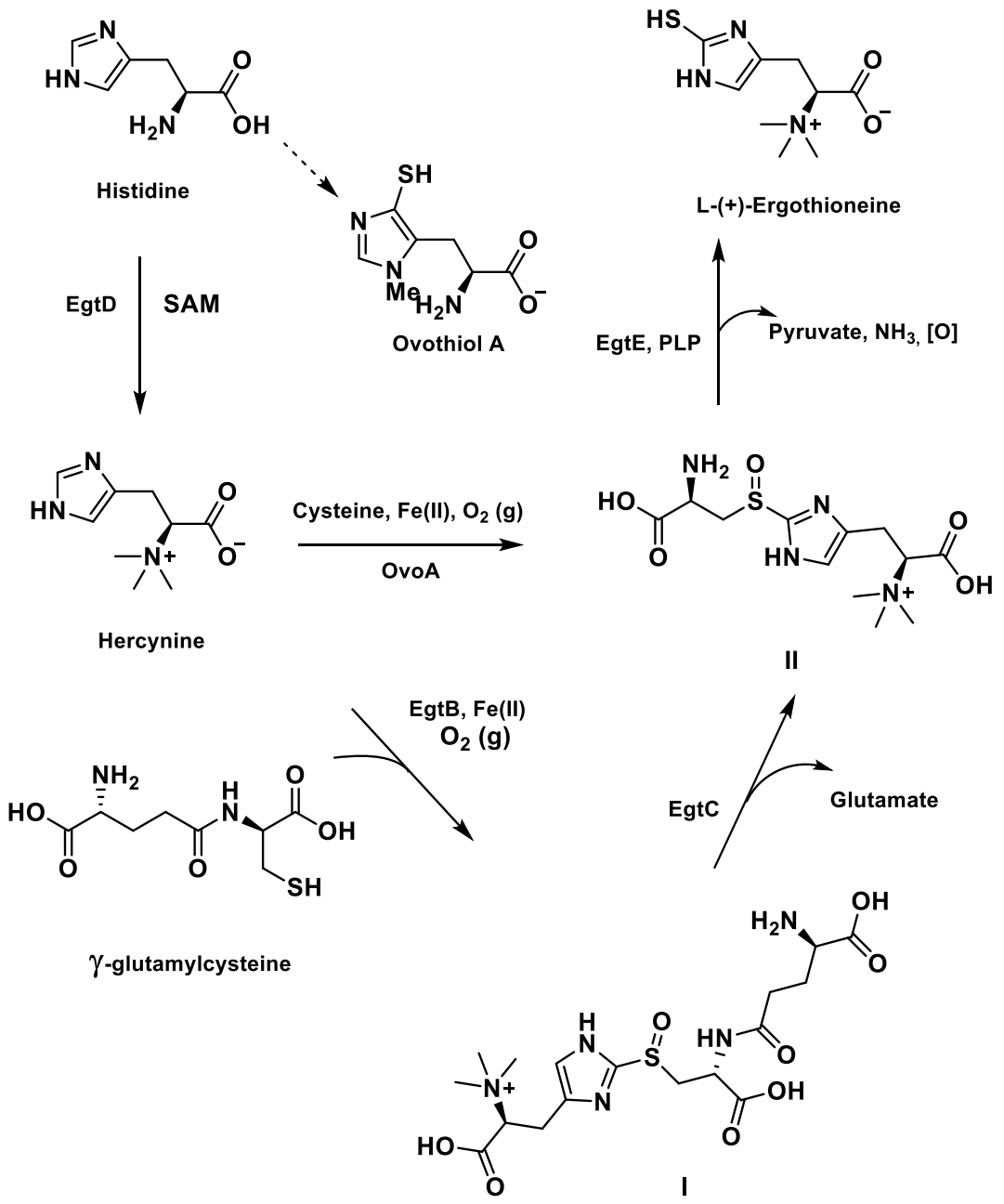

Scheme 2.1. *Biosynthetic pathway of L-(+)-ergothioneine in microorganisms. I = γ-glutamylcysteinyl hercynine; II = S-(β-amino-β-carboxyethyl)ergothioneine sulfoxide. Ovothiol A (N1-methyl-4-mercaptohistidine) is a natural thiohistidine regio-isomer of ergothioneine, a highly reducing antioxidant which accumulates to very high levels in the eggs of certain marine invertebrates.*

An interesting parallel exists with OvoA, a homolog of EgtB that is involved in the synthesis of ovothiol A. Like EgtB, OvoA is an iron (II)-dependent sulfoxide synthase; however, the two enzymes exhibit distinct substrate specificities.

OvoA exclusively uses L-cysteine as its sulfur donor and histidine as a co-substrate, whereas EgtB requires γ-glutamylcysteine as the sulfur donor and hercynine as the co-substrate. Furthermore, OvoA demonstrates a unique sulfurization pattern on the imidazole ring of histidine, which shifts from the δ-carbon to the ε-carbon depending on the degree of α-*N*-methylation.

Notably, OvoA can directly convert hercynine into *S*-(β-amino-β-carboxyethyl)ergothioneine sulfoxide (II), though it also produces a minor amount of δ-sulfoxide (the ovothiol substitution pattern) when α-*N,N*-dimethylhistidine is used as a co-substrate.

Although functional forms of EgtB and EgtC have been successfully expressed and studied over the years, the structure of EgtE has been recently elucidated.[25] The biosynthesis of intermediate substrates still presents challenges for more detailed investigations. This limited availability has constrained the comprehensive characterization of these enzymes, leaving some mechanistic details open for further research.

The production of EGT faces numerous challenges in both its biosynthesis and chemical synthesis, primarily due to the structural complexity of the molecule and the specificity required at each step of its production.

Biosynthetically, the pathway involves a series of highly specialized enzymes (EgtA, EgtB, EgtC, EgtD, and EgtE), each of which performs precise reactions that are difficult to replicate or manipulate for large-scale production. The strict substrate specificity of these enzymes, particularly EgtB and EgtE, makes it challenging to engineer the pathway in heterologous systems, as each intermediate must be synthesized and utilized with high precision. Moreover, key enzymes such as EgtE have proven elusive in functional studies, with significant difficulties in expression and substrate availability further hindering progress. The lack of readily available intermediates, such as γ-glutamylcysteinyl hercynine, also limits research and industrial applications, as these intermediates are crucial for studying the catalytic mechanisms of the enzymes.

To address these limitations, recent research has focused on the development of genetically modified microorganisms capable of producing ergothioneine more efficiently. As reported by Sato et al. (2025), the heterologous expression of fungal biosynthetic genes, such as *egt1* and *egt2* from *Neurospora crassa* and *Claviceps purpurea*, in yeast species like *Saccharomyces cerevisiae* and *Yarrowia lipolytica* has led to the creation of microbial strains with significantly improved productivity.[26] These strains have been optimized not only by introducing multiple gene copies but also by engineering the host metabolism to enhance the availability of critical precursors such as L-histidine, L-cysteine, and γ-glutamylcysteine. In some cases, the fermentation yield has reached gram-per-liter levels, highlighting the great potential of synthetic biology for enabling sustainable and scalable ergothioneine production. These advances represent a promising route to overcome the biosynthetic bottlenecks and pave the way for the industrial application of EGT in the pharmaceutical, cosmetic, and nutraceutical sectors.

Chemical synthesis

Sulfur-containing amino acids, such as cysteine and methionine, are fundamental components of biological systems and play essential roles as building blocks of proteins. The presence of sulfur in their structures, either as a thiol group in cysteine or as a thioether in methionine, is crucial for their redox activity and physiological functions.[27]

These sulfur-containing fractions enable critical biochemical processes, including maintaining cellular redox balance, facilitating enzymatic catalysis, and contributing to the structural stability of proteins through disulfide bond formation. Moreover, their redox-active nature makes them indispensable in protecting cells from oxidative damage and participating in signalling pathways that regulate cellular homeostasis. The widespread distribution and versatility of these amino acids underscore their importance and their indispensable role in life processes.[28]

Another group of sulfur-containing amino acids includes thiohistidine derivatives, such as 2-thiohistidine and *L*-ergothioneine. In these compounds, sulfur is integrated into a unique imidazole-2-thione structure, distinguishing them from the more ubiquitous thiol- and thioether-based amino acids like cysteine and methionine (**Figure 2.1**). This structural feature imparts distinct chemical and biological properties, including exceptional redox stability and the ability to act as potent antioxidants.[29]

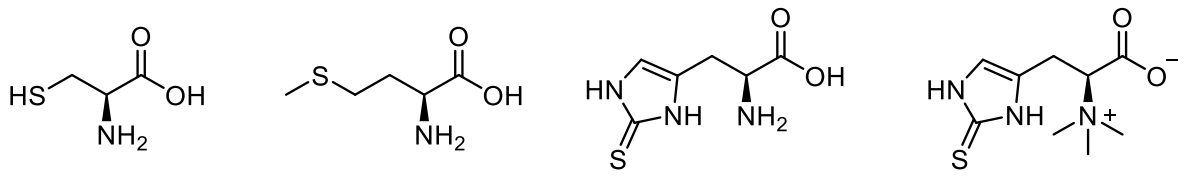

Cysteine Methionine 2-thiohistidine L-ergothioneine

***Figure 2.1**. Sulfur-containing amino acids.*

The discovery of L-ergothioneine as a potentially new vitamin has significantly stimulated the search for sustainable synthetic routes and further exploration of thiohistidine derivatives.

Despite their seemingly simple structures, the selective introduction of sulfur on histidine poses considerable synthetic challenges. The process necessitates the protection of competing reactive sites, including the carboxyl and amino groups, to avoid undesired side reactions. This requirement significantly increases the number of synthetic steps and involves the extensive use of organic solvents, gaseous HCl, and chromatographic purifications.

The synthesis of 2-thiohistidine and L-ergothioneine has been accomplished using different methodologies, both involving sulfur reagents and protective groups. For 2-thiohistidine, 5–7 steps are required depending on the route chosen[30]. The synthesis of ergothioneine involves 9–10 steps, given the additional complexity of establishing its unique trimethylammonium functionality.[12] The necessity of protecting groups, especially for the nucleophilic sulfur during critical stages, adds to the complexity of the procedure.

While the use of protecting groups has been essential in the past to ensure selectivity and minimize undesired side reactions, these methods often involve lengthy procedures, require additional reagents, and generate excess waste, reducing their overall efficiency and sustainability. As a result, modern research in synthetic chemistry has increasingly focused on protecting-group-free methodologies, which hold immense potential to simplify reaction processes, enhance cost-effectiveness, and improve the environmental sustainability of chemical syntheses.

One of the most promising advancements in this area is the shift toward water-based reactions, which not only eliminate the need for protecting groups but also capitalize on the unique reactivity of water.[12] The so-called "on-water effect", which accelerates reaction rates in aqueous systems, has further demonstrated the practicality of this approach, often enabling simplified product purification and isolation steps.[31]

Considering these developments, Erdelmeier and colleagues in 2012 introduced a groundbreaking biomimetic synthesis of L-ergothioneine starting from hercynine, which exemplifies this new paradigm.[12]

This strategy leverages the inherent advantages of protecting-group-free synthesis in water, employing cysteine as a sustainable and readily accessible sulfur source. Cysteine, being both renewable and environmentally friendly, provides an efficient means of introducing sulfur into the molecule while maintaining high selectivity under mild conditions.

The method not only eliminates the need for intermediate protection and deprotection steps but also aligns with the principles of green chemistry, offering a scalable route to sulfur-containing amino acids, including L-ergothioneine and various thiohistidine derivatives.

The approach described by Erdelmeier et al. represents a significant leap forward in the field, rendering these previously challenging compounds readily accessible in multi-gram quantities for further biological investigations.

By combining the benefits of protecting-group-free synthesis with the reactivity-enhancing properties of water, this study sets a new standard for the efficient and sustainable production of biologically relevant sulfur-containing compounds.

The synthesis begins with the reaction of L-hercynine with liquid bromine, forming a bromolactone intermediate. This intermediate is then subjected to a regioselective substitution with cysteine, which introduces the sulfur atom into the structure, thereby forming a cysteine-conjugated intermediate.

The next step involves a thermal cleavage reaction, where thiols facilitate the cleavage of the intermediate, resulting in the formation of L-ergothioneine. The whole process is shown in **Scheme 2.2**.

This two-step, one-pot process occurs in water and eliminates the need for protecting groups, significantly streamlining the synthesis while reducing the number of reactions and the overall complexity compared to previous methods. A key aspect of the study is the evaluation of alternatives to liquid bromine, which is often used in these types of reactions but is a hazardous and challenging reagent to handle. The authors explore several safer methods for generating bromine or hypobromous acid (HOBr) in situ, which would allow for the same bromination step without the risks associated with liquid bromine. Preliminary findings suggest that these alternatives are viable, offering a safer and more sustainable approach to the synthesis of L-ergothioneine.

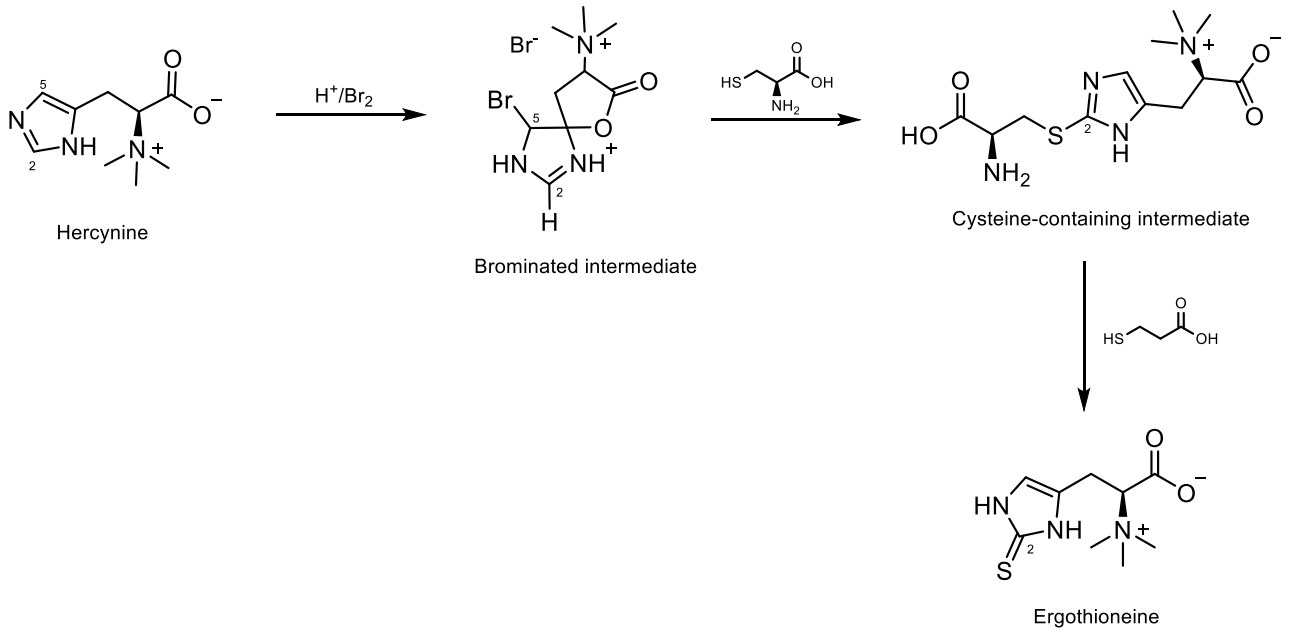

Scheme 2.2. *Synthesis of L-ergothioneine starting from hercynine.*[12]

Building on the earlier work in which cysteine was employed as a sulfur donor for the synthesis of L-ergothioneine, a new chemical synthesis was developed by Daunay et al. that further utilizes cysteine in a novel manner.[32] This method provides a simple and efficient pathway to L-ergothioneine in multi-gram quantities and extends to the entire family of 2-thiohistidine derivatives.

The process begins with the activation of hercynine or histidine derivatives using bromine, followed by reaction with cysteine to form a thioether. This thioether can then be easily cleaved to yield ergothioneine and thiohistidine derivatives. In this study, alternatives to cysteine as a sulfur donor were explored, with thioacetic acid emerging as a potential candidate. Thioacetic acid as a thiol source was 1st reported in the Khonde-Jardine patent W**O2016046618A1,** WIPO (PCT). However, unlike cysteine, which reacts with the bromolactone intermediate at the 2-position, thioacetic acid reacts at the 5-position, forming a thioester instead (**Scheme 2.3a**). This unexpected reactivity provides a new route to the synthesis of 5-sulfur-substituted histidine derivatives, which were previously not accessible via traditional chemical synthesis methods involving C–S bond formation.

Furthermore, the same preference for 5-substitution by thioacetic acid was observed when *N*-bromosuccinimide (NBS) was used instead of bromine to activate histidine (**Scheme 2.3b**).

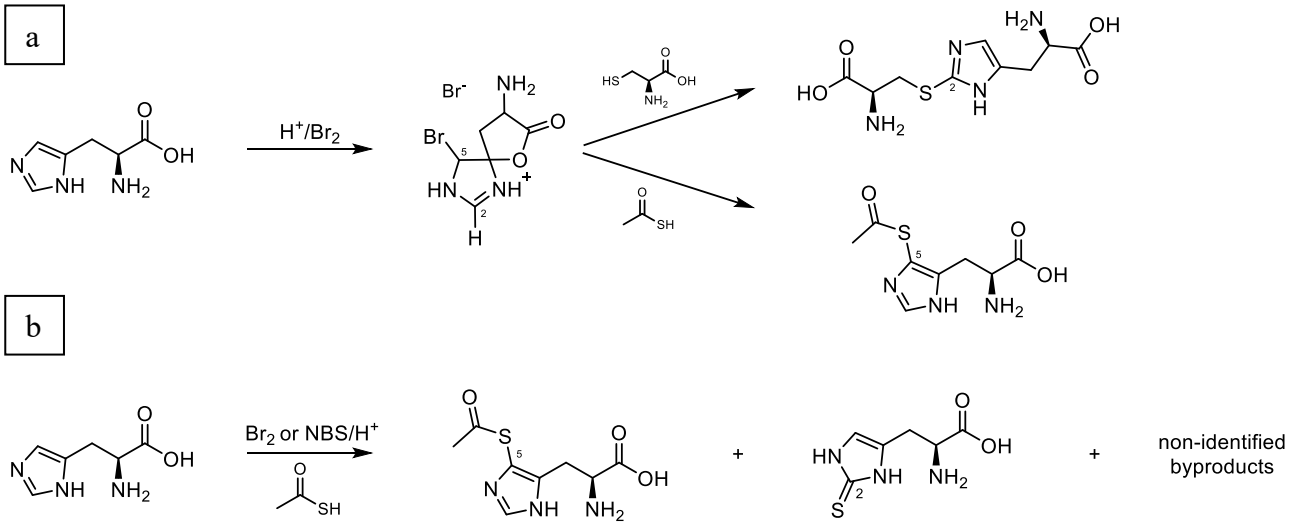

Scheme 2.3. *a) Discovery of a regioselectivity switch using thioacetic acid. b) Reaction of activated L-histidine with thioacetic acid using NBS.*

Rationale of the study

In previously reported syntheses of ergothioneine, aqueous hydrochloric acid (HCl) has been consistently employed as solvent due to its ability to dissolve both organic and inorganic reactants and to activate brominating agents such as bromine or N-bromosuccinimide (NBS). The acidic medium facilitates halogenation and subsequent thiolation of hercynine, leading to sulfur-containing amino acids. However, these procedures often result in complex mixtures and modest yields, and the neutralization step introduces desalting challenges that complicate purification.

Bromination of the imidazole ring is a key step in ergothioneine synthesis, and the position of substitution (C-2 or C-5) depends strongly on reaction conditions and the thiolating agent used. Thioacetic acid typically promotes 2-thiolation, whereas cysteine favours 5-thiolation. Regioselectivity is also influenced by solvent polarity, pH, and activation mode (electrophilic versus radical). Recent studies have demonstrated that visible-light-activated NBS bromination using organic dye catalysts such as Rose Bengal can proceed efficiently under mild, non-acidic conditions.

At low pH under aqueous conditions, bromination of the imidazole ring of histidine, generally occurs through an electrophilic aromatic substitution mechanism. The specific position on the imidazole ring where bromination occurs depends on various factors, including the pH of the solution, the presence of other substituents, and the reaction conditions.

The free radical bromination of histidine involves bromination at the allylic-like benzylic position of the imidazole ring—specifically, the C-5 position on the ring (if no side chain bromination dominates). The reaction generally uses NBS under radical conditions (heat or light) and often proceeds via a radical substitution mechanism.

Functionalized indazoles were brominated in moderate to excellent yields using NBS under visible-light activated conditions. The authors reported the screening of organic dye catalysts resulting in the identification of rose bengal as the most efficient catalyst to use with NBS toward indazoles.[33]

Further inspiration by the literature is the report of halogenation of histidine esters in ACN.[34] It has also been reported that *N*-halosuccinimides are better halogenating agents for bioimidazoles, and acetonitrile is the solvent of choice for these reactions.[35]

Reported halogenation of histidine esters supports bromination at the C-5 position and not at the C-2 unless complete consumption of the brominating agent.[34,35,36] Any access brominating agent leads to double bromination at C-2 and C-5, but no bromination is recorded at position C-2 only (**Figure 2.2**).

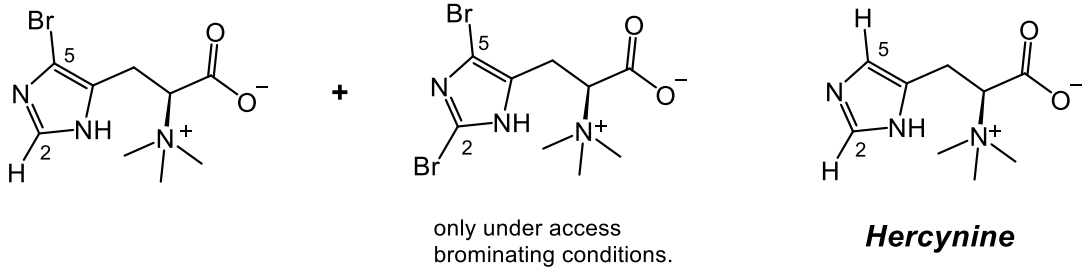

Figure 2.2. *Possible brominated reaction intermediates following the first step of the reaction. No C-2 mono-brominated product is possible according to literature precedence.*

In most cases, halogenation reactions were carried out for 24 h at room temperature in the absence of light which was the conditions considered for the bromination of hercynine. Accordingly, acetonitrile (ACN) was selected as the solvent for the reaction, replacing the conventional aqueous acid solution. Acetonitrile was chosen for several reasons.

Firstly, as a polar aprotic solvent, acetonitrile offers good solubility for a wide range of organic and inorganic compounds, including those involved in the reactions under study. This feature is particularly important in reactions that require a neutral or non-aqueous environment to minimise side reactions or undesired protonation events. Secondly, acetonitrile's relatively low dielectric constant compared to water can alter the solvation dynamics of the reaction intermediates, potentially influencing the reaction pathway. This could change the reactivity of the reagents and intermediates, potentially improving the efficiency and selectivity of the reactions.

Additionally, acetonitrile is known to be a less corrosive and more stable solvent compared to aqueous hydrochloric acid, which could offer advantages in terms of safety and ease of handling during large-scale or prolonged reactions.

Finally, acetonitrile has a relatively low boiling point of 81.6°C, which is a crucial requirement for its easy removal at the end of the reaction. This characteristic makes it particularly advantageous in synthetic procedures, as it can be efficiently evaporated under reduced pressure, minimizing residual solvent contamination in the final product. In the context of the present study, the low boiling point of acetonitrile aligns well with the objectives of optimizing the purification process for ergothioneine derivatives. Its volatility reduces the energy requirements for solvent removal, contributing to a more sustainable and efficient workflow. Furthermore, the reduced boiling point aids in preserving the stability of thermally sensitive intermediates or final products during the evaporation step. This property, combined with its suitability as a solvent for polar and organic compounds, underscores acetonitrile as a solvent of choice for this synthetic methodology.

A further motivation was to investigate the possibility of more favourable thiolation at the C-2 position of the imidazole ring with ACN as solvent. These experiments aimed to evaluate whether this solvent could provide similar or improved results compared to the traditional aqueous HCl system.

The focus was placed on optimizing the reaction conditions, including the influence of light exposure and the duration of the bromination step, as well as refining the downstream purification methods. Specifically, the effect of conducting the reaction under light (using lamps emitting light at specific wavelengths) versus in the dark was considered.

Additionally, different reaction times for the bromination step (first step of the reaction) were considered, ranging from several hours to an overnight reaction, in order to determine the optimal conditions for the activation of the halogenating agent.

In terms of purification, different chromatographic techniques were investigated in the past which included both normal-phase and reverse-phase chromatography columns. While considered as a last resort for scale up, chromatographic methods were still considered to improve the purity of the final products, considering that solvent choice and column type can significantly affect separation efficiency and product yield. Furthermore, solid-liquid and liquid-liquid extraction procedures were considered as a more sustainable option to concentrate the products of interest. This focus on solid-liquid extraction techniques was aimed at optimizing the recovery of the desired compound with the knowledge that the polar product is water soluble, while reagents were mostly soluble in organic solvents.

By comparing the efficiency, selectivity, and product distribution obtained with acetonitrile to those achieved using aqueous HCl, the study aims to determine whether acetonitrile can serve as a viable alternative that enhances the synthetic process or offers distinct advantages in terms of reaction control, safety, and environmental impact. The various modifications to reaction conditions and purification processes also offer valuable insights into how acetonitrile can influence the overall reaction mechanism and yield, further contributing to the ongoing efforts to optimize and refine chemical synthesis methods.

Aims and Objectives

Based on the above rationale, this study aimed to develop a greener and more efficient synthetic approach to ergothioneine derivatives by investigating alternative solvent systems and reaction conditions.

The specific objectives were:

- To evaluate acetonitrile (ACN) as a non-aqueous alternative to aqueous HCl in the bromination and thiolation of hercynine.
- To assess the regioselectivity of bromination at the C-2 and C-5 positions under modified conditions.
- To compare the reactivity of different thiolating agents (thioacetic acid and cysteine) in promoting selective C–S bond formation.
- To study the influence of light activation (visible-light irradiation using Rose Bengal) and reaction time on bromination efficiency.
- To optimize purification methods, focusing on sustainable solid–liquid extraction techniques for polar thiolated products.
- To compare overall yield, selectivity, and environmental impact of the ACN-based system versus the conventional aqueous HCl method.

Results and Discussion

This study aimed to develop an efficient synthesis for producing ergothioneine derivatives by investigating different reaction conditions and perfecting purification procedures. Although an introduction to the synthetic approaches was presented in the previous chapter, it is essential to outline the rationale for the modifications introduced in this chapter.

The focus was on searching for the most favourable conditions to obtain the desired product with maximum purity, while minimizing impurities and by-products. The following paragraph outlines the general synthetic strategy adopted, which was subsequently modified to improve reaction efficiency and selectivity. The reaction conditions were adjusted based on preliminary results and then optimized by modifying the reaction time, the solvent used in each step and the purification methods in order to achieve better results.

The synthetic strategies were based on a bromination reaction of hercynine in acetonitrile using NBS as a brominating agent and Rose Bengal as a photocatalyst.[33,37] Hercynine was obtained from a prior synthesis in the lab. The role of light in photocatalytic reactions of this type is crucial, as it activates the photocatalyst, in this case, Rose Bengal, by promoting it to an excited singlet or triplet state. The excited photocatalyst then transfers energy to the brominating agent, facilitating homolytic cleavage of NBS and generating reactive bromine radicals. These radicals can subsequently engage in selective bromination of the substrate.

The synthesis of L-5-acetylsulfanyl-α-*N,N,N*-trimethyl-histidine (**3a**) and/or L-2-acetylsulfanyl-α-*N,N,N*-trimethyl-histidine (**4a**) was conducted in a two-step, one-pot process and is shown in **Scheme 2.4a**. The first step involved the bromination of hercynine **1** in ACN using NBS as the brominating agent at room temperature, leading to the formation of the bromolactone intermediate **2**. Subsequently, the regioselective addition of the sulfur donor introduced an S-acetyl group at the C5 (and/or C2) position of the imidazole ring, yielding compound **3a (**and/or **4a)**.

Extensive purification was required to remove residual succinimide and NBS, though these steps were not entirely effective in reducing their presence.

The purification process included column chromatography, liquid-liquid extraction and solid-liquid extraction. The treatment of compound **3a and 4a** with 3-mercaptopropionic acid at 90-100°C for 18 hours induces a thermal cleavage reaction, where thiols facilitate the cleavage of the intermediate, resulting in the formation of compound **3b** and L-ergothioneine **4b**.[32] The latter deacetylation step was not conducted in this study.

Daunay, et al reported a minor 2-thiolation of histidine which encouraged the endeavour a similar expectation in the thiolation of hercynine.[32] An ideal outcome would be a separable mixture of two products, one substituted at position 5 (which is refer to as **3b**, as shown in **Scheme 2.4b**) and one substituted at position 2 (ergothioneine, **4b**).

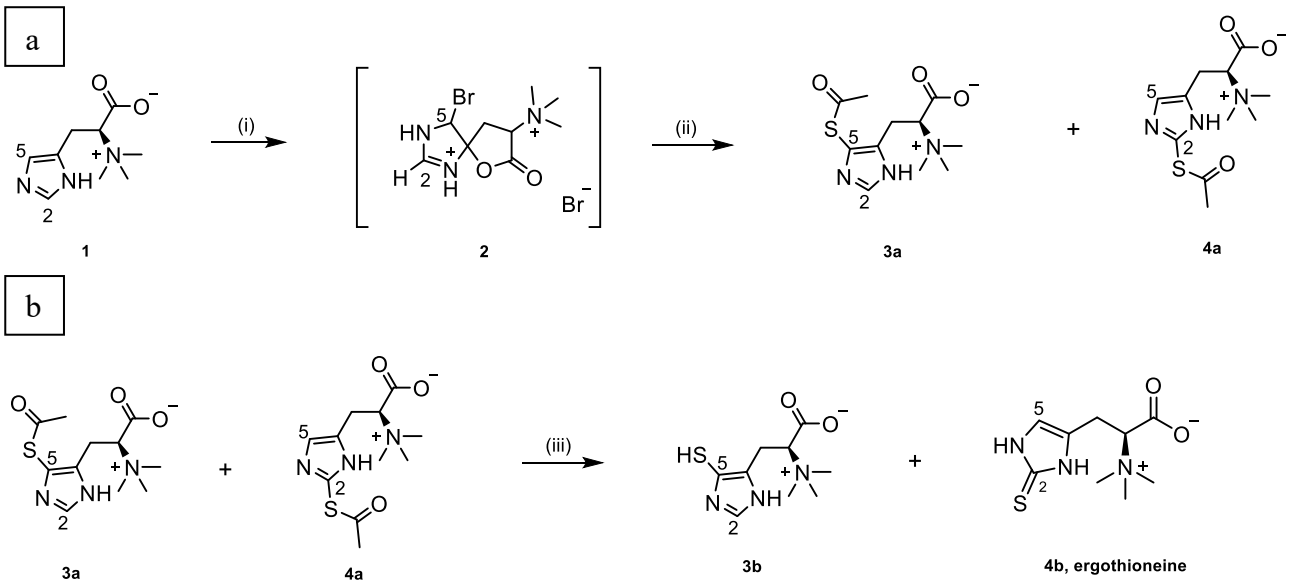

Scheme 2.4. *Reaction scheme of the synthesis of L-5/2-acetylsulfanyl-α-N,N,N-trimethyl-histidine. a) Reagents and conditions: (i) CH_3CN / NBS / Rose Bengal / r.t. / the duration of this step was optimized and varied across different experiments, (ii) sulfur donor, thioacetic acid, selected based on the specific reaction conditions, b) Mixture of two products,* ***3a*** *and* ***4a*** *deacetylated by (iii) 3-mercaptopropionic acid / 90-100°C / 18h.*

Photochemical activation (Reactions 1-6)

The first reactions (reactions 1-6, shown in **Scheme 2.5**) were conducted under illumination at 450 nm or 495 nm, followed by the addition of Boc-protected cystine or thioacetic acid in the second step.

The Boc-protected cystine and thioacetic acid were utilised to generate an acetonitrile-soluble thiyl radical as the thiolating agent.

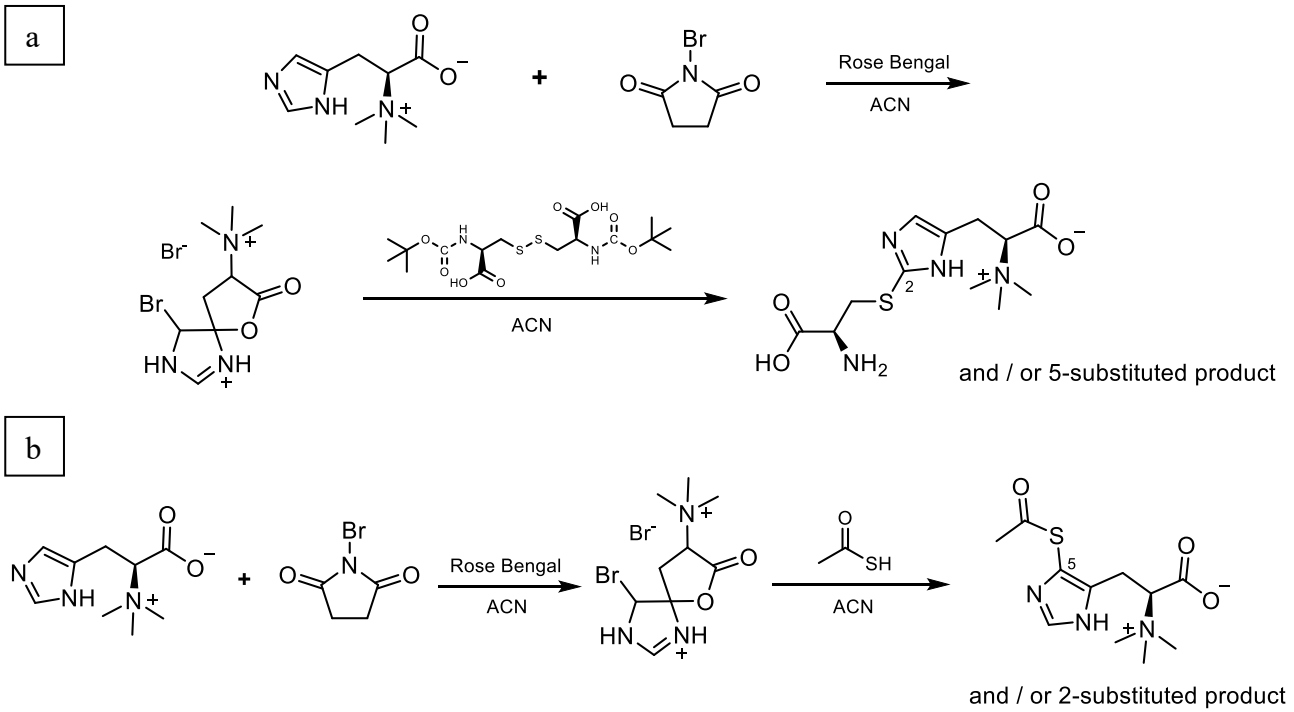

***Scheme 2.5**. a) Photochemical reactions 1, 3, 5 and 6: Synthesis of 3-{2-[(2-amino-2-carboxyethyl)thio]-1H-imidazol-4-yl}-2-(trimethylammonio) propanoate. b) Photochemical reactions 2 and 4: Synthesis of L-5-acetylsulfanyl-α-N,N,N-trimethyl-histidine.*

The reaction conditions used for the syntheses (Reactions 1-6) are shown in **Table 2.1**.

***Table 2.1**. Reaction conditions used for the synthesis 1-6.*

Reaction	***Wavelength of the lamp (nm)***	***Sulfur donor***	***Duration of the bromination step***
1	495	Boc-cystine	20 minutes
2	495	Thioacetic acid	20 minutes
3	450	Boc-cystine	20 minutes
4	450	Thioacetic acid	20 minutes
5	495	Thioacetic acid	1 hour
6	495	Thioacetic acid	Overnight

In these reactions, hercynine was dissolved in acetonitrile and reacted with NBS and Rose Bengal followed by the addition of the sulfur donor. A TLC analysis was performed to monitor the reaction progress.

For reactions 1–4, the reaction with boc-cystine did not proceed, as indicated by TLC analysis, which showed only unreacted hercynine. This may be due to the limited solubility of boc-cystine in acetonitrile. However, product spots formed upon consumption of hercynine after the addition of thioacetic acid. The identical TLC profiles of reactions 2 and 4 suggest that the same transformation occurred in both cases, implying that the light wavelength was not a determining factor in the reaction outcome. NMR analysis confirmed the absence of the desired product.

Various factors might have contributed to the failure of these reactions. Although the excitation wavelength of Rose Bengal is known, the light source used may not have provided sufficient intensity at that specific wavelength, leading to incomplete photocatalyst activation. Additionally, the presence of solvents or reaction intermediates could have quenched the excited state of the photocatalyst before effective radical generation occurred, reducing the overall efficiency of the reaction.

The formation of by-products (TLC) suggests that undesired radical pathways were also active, potentially leading to non-selective bromination or degradation of the starting material.

Finally, if NBS did not effectively undergo homolytic cleavage under the given conditions, the formation of bromine radicals may have been limited, reducing the bromination efficiency. To overcome the limitations observed in the initial reactions, a series of new experimental conditions was tested across multiple reactions.

For reactions 5 and 6 an increased concentration of reagents was introduced while maintaining the reaction conditions under irradiation with a 495 nm lamp. Following the bromination step, the acetonitrile solvent was evaporated, and an aqueous hydrochloric acid solution was introduced before adding thioacetic acid.

This adjustment was made after the observation that hercynine did not fully dissolve in acetonitrile, which could have affected the efficiency of the second step. While previous studies from the literature have always used aqueous HCl for these reactions, the goal was to reduce the use of this solvent due to the challenge of removing it downstream by replacing it, at least partially, with acetonitrile. The initial plan was to carry out the entire reaction in acetonitrile (as done in reactions 1-4). Since hercynine was not completely soluble, this warranted a modification to the approach by introducing aqueous HCl in the second step. Despite this adjustment, using acetonitrile in the first step still represents an improvement over fully aqueous conditions and reduces the amount of hydrochloric acid required.

The reaction mixtures were subsequently neutralized with ammonia to adjust the pH to 4–5, then frozen, and subsequently subjected to lyophilization overnight. The resulting dry samples were subjected to solid-liquid extraction using ethyl acetate followed by ethanol.

Ethanol was employed to facilitate the removal of Rose Bengal from the reaction mixture due to its solubility in this solvent. This approach aimed to selectively eliminate Rose Bengal and other undesired byproducts while preserving the target compounds in the mixture.

In the aromatic region, two distinct signals were observed with integral values of 1 proton each. A product substituted at position 2 of the imidazole ring is consistent with L-5-acetylsulfanyl-α-*N,N,N*-trimethyl-histidine (**3a**) whereas the other does not exhibit any corresponding upfield signals for a 5-substituted product.

Comparison of the aromatic resonances of the NMR spectra of samples 5 and 6 with that of hercynine reveals a noticeable shift in signal positions, indicating that the obtained product does not contain unreacted hercynine, as shown in **Table 2.2** and **Figure 2.3**.

Table 2.2. *Aromatic peaks of hercynine compared to products of reactions 5 and 6 (NMR solvent: D_2O).*

NMR spectra	***δ_{H2} (ppm)***	***δ_H (ppm)***
Hercynine	7.81	7.01 (H5)
Reaction 5	8.59	7.22 (unknown)
Reaction 6	8.56	7.22 (unknown)

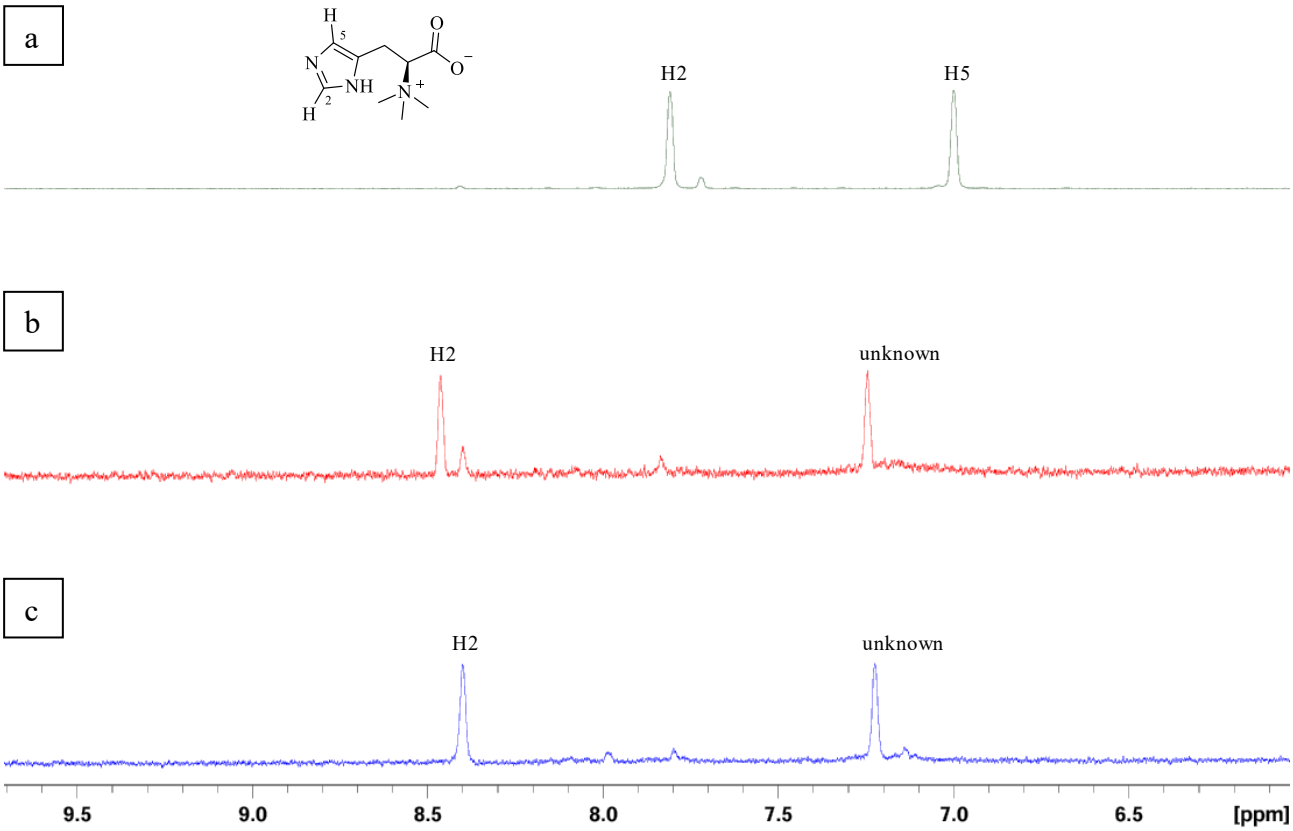

Figure 2.3. *NMR spectra representing the aromatic region of (a) hercynine, (b) 1hr post addition of thioacetic acid, a mixture of two products, one substituted at position 2, δ 8.49 ppm, and the other unidentified at δ 7.22 (c) a mixture of two products, one substituted at position 2 δ 8.4 ppm and the other unidentified at δ 7.22 for reaction 6.*

After the solid-liquid extraction, each fraction was divided into two equal aliquots. Each aliquot was treated as shown in the flow diagram in **Figure 2.4**.

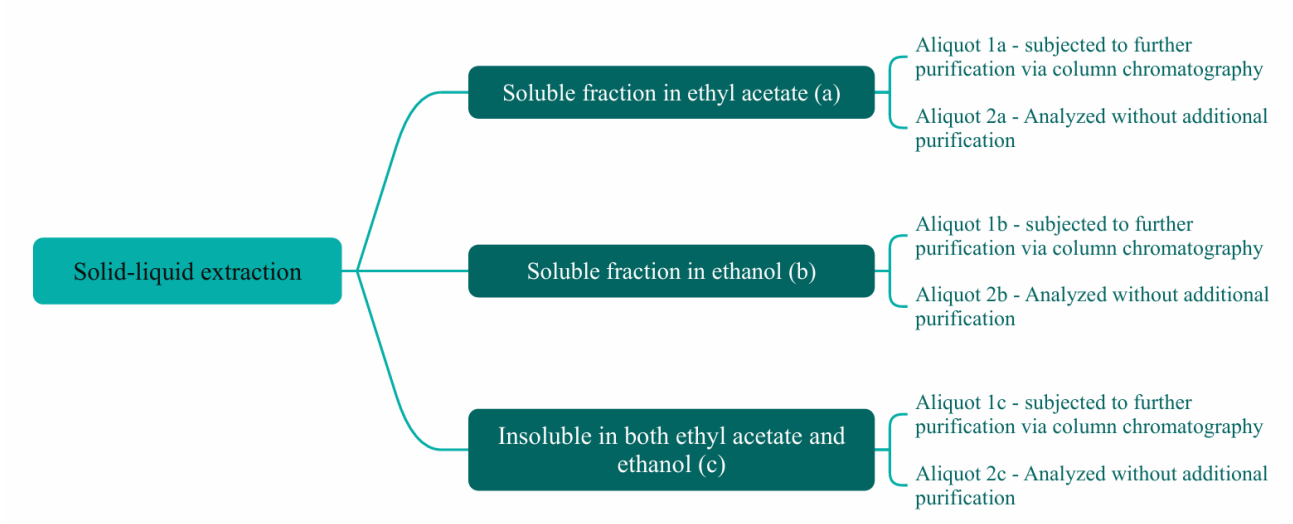

Figure 2.4*. Further purification after solid-liquid extraction.*

Proton NMR obtained from the ethyl acetate extract showed only very minor amounts of targeted product (*aliquots 1a and 2a*) (**Figure 2.4**), the focus subsequently shifted to the aliquots subjected only the solid fraction without additional purification, i.e., *aliquots 1b* and *2b*.

NMR analysis revealed that the spectra obtained after silica column purification were significantly less pure than those of the aliquots that underwent only solid-liquid extraction. These findings suggest that, while silica column chromatography was effective in eliminating certain contaminants, it is not a suitable method for isolating our target compound.

Due to its high polarity, the compound elutes rapidly in reverse phase and is not adequately retained by the chromatographic medium, specifically C-18. Moreover, chromatographic purification is inherently time-consuming and limiting in scalability. Therefore, alternative purification strategies were explored and systematically evaluated against column chromatography to assess its relative effectiveness in isolating the desired product.

Despite the persistence of unreacted reagents, the quality of the NMR spectra obtained from these fractions showed significant improvement compared to previous attempts.

Furthermore, these experiments provided insights into the extraction process. While ethyl acetate proved effective in removing certain impurities, it was not capable of extracting the target compound which is present as the 5-substituted thioacetate. Instead, the desired product mixture was successfully recovered through solid-liquid extraction using ethanol.

The spectrum shown below, **Figure 2.5**, corresponds to the *aliquot 2b* (fraction soluble in ethanol), which results in a cleaner spectrum which became the focus in the purification strategy. Since the NMR spectra of reactions 5 and 6 exhibit the same pattern, only the NMR spectrum of reaction 6 is shown in **Figure 2.5**. A comparison of the NMR spectra of reactions 5 and 6 is shown in Chapter 4, "*Experimental*", **Figure 4.1**.

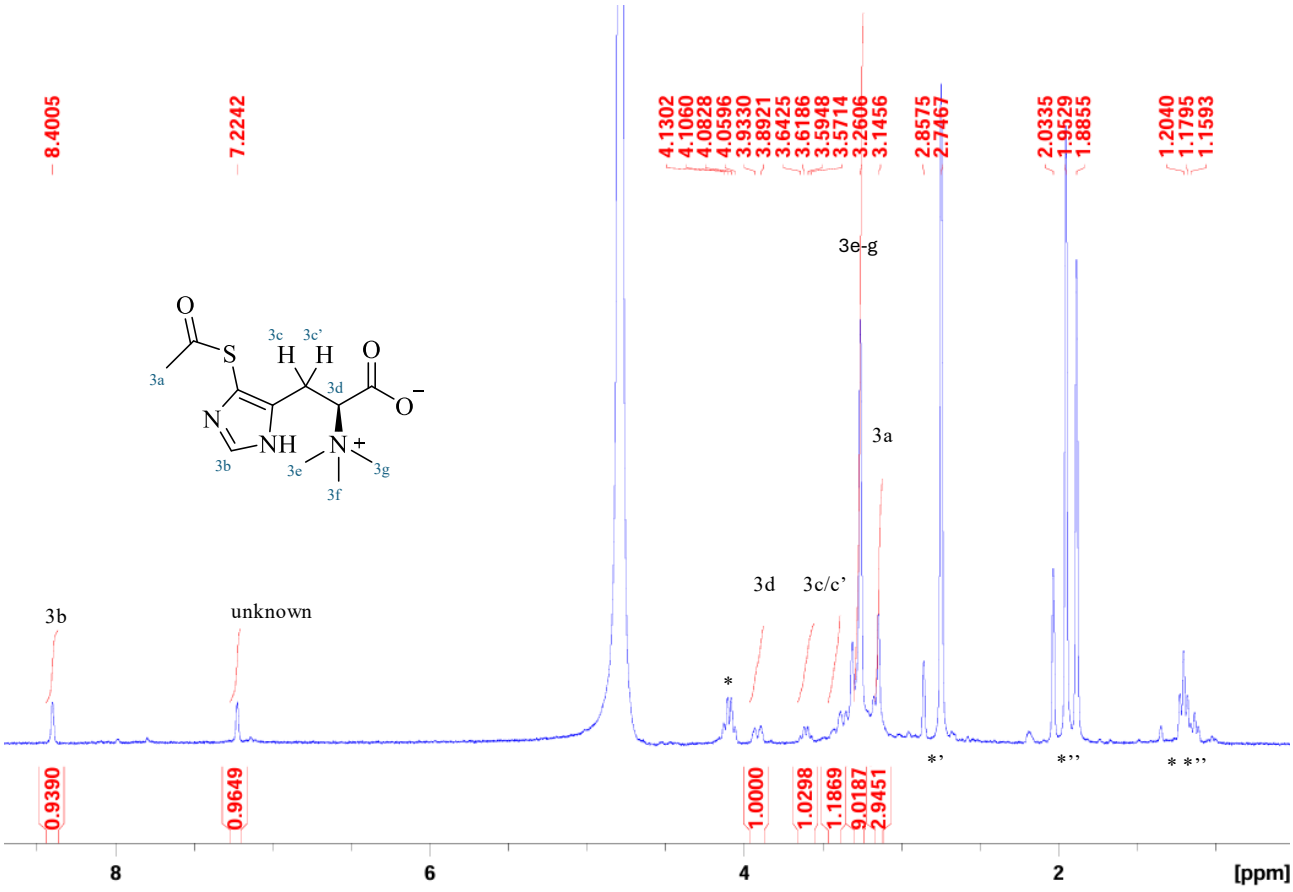

Figure 2.5. *^{1}H NMR spectra of reaction 6. D_2O is used as the solvent.*

** traces of ethanol.*

**' traces of NBS and succinimide.*

**" traces of residual acetonitrile, incomplete evaporation of acetone or traces of ethyl acetate (all of which were used at different stages of the reaction and purification process).*

All unassigned peaks in the NMR spectrum can be attributed to reaction by-products and residual solvents which proved to be difficult to remove under high vacuum overnight. The signals observed around 2.9 and 2.7 ppm correspond to unreacted NBS and succinimide, respectively, both of which are expected by-products of the reaction. The main objective of this project is to refine the purification method to effectively remove these residues.

Finally, NMR analysis indicated that while variations in bromination time did not initially appear to significantly influence the reaction outcome, subsequent experiments, which will be discussed in this chapter, revealed that a longer bromination period were more beneficial.

Although other factors, such as reagent concentration, solvent choice, or reaction mechanism, certainly play a role in the overall reaction efficiency, extending the bromination time proved to be beneficial for achieving a more complete transformation in the first step.

As reactions 1-4, the quantities of reactants used in reactions 5 and 6 were minimal, primarily to evaluate the behaviour on TLC and to obtain a sufficient amount of material for NMR analysis. Therefore, the yields were not determined.

Reactions in the dark (7-10)

Reactions 7-10 explored additional variations in reaction parameters, shown in **Table 2.3**.

Table 2.3. *Reaction conditions used for the synthesis 7-10.*

Reaction	***Light conditions***	***Sulfur donor***	***Duration of the bromination step***	***Rose Bengal***
7	Dark	Thioacetic acid	1 hour	Yes
8	Dark	Thioacetic acid	1 hour	No
9	Dark	Thioacetic acid	Overnight	Yes
10	Dark	Thioacetic acid	Overnight	No

Reactions 7–10 followed the same procedure as reactions 5 and 6. After the first step of reaction, the acetonitrile was evaporated, and an aqueous HCl solution was added, followed using thioacetic acid as sulfur donor. The reaction mixture was then neutralized with ammonia, frozen, and subjected to lyophilization.

These experiments aimed to elucidate the role of light activation and reaction duration in product formation. The attempt to eliminate the use of the photocatalyst, Rose Bengal, was made because in previous experiments, it was very difficult to remove it.

Additionally, it imparted a strong pink coloration to the solution, which hindered the ability to monitor the changes in colour at different reaction steps.

From the spectra of reactions 5 and 6, it was observed that the duration of the first reaction step did not appear to be a determining factor. However, extending the duration of the first bromination step could lead to better conversion of the reagents into products, thereby reducing the amount of unreacted NBS.

Subsequent purification steps, including solid-liquid extraction and column chromatography on a C18 reversed-phase column, revealed that reaction 10 provided the best results in terms of product purity. The NMR spectrum of this reaction product is shown in **Figure 2.6**.

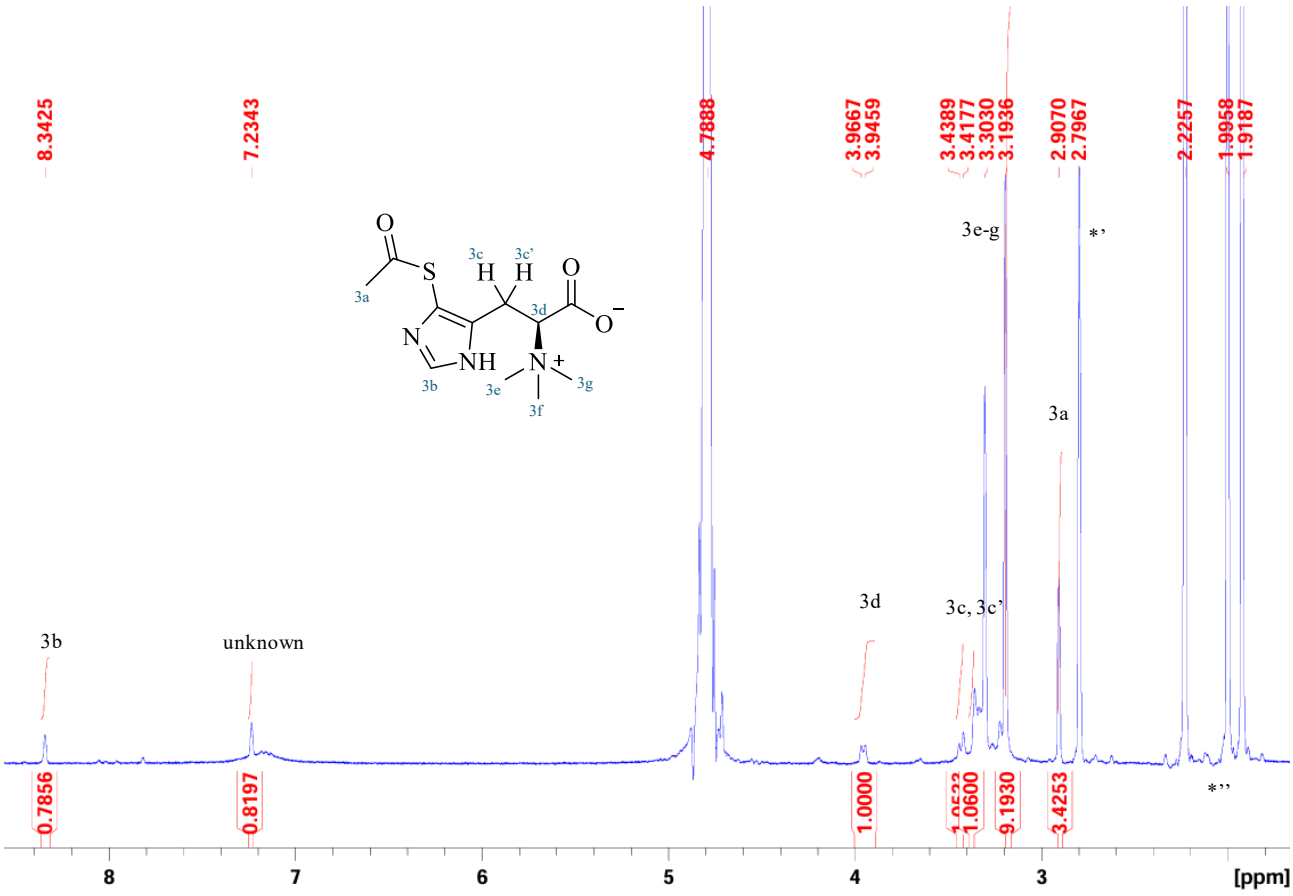

Figure 2.6. *NMR spectra of the product of reaction 10. D_2O is used as the solvent.*

**' traces of succinimide.*

**" traces of residual acetonitrile, incomplete evaporation of acetone or traces of ethyl acetate (all of which were used at different stages of the reaction and purification process).*

Two resonances were still visible in the aromatic region (unknown at δ7.23 ppm), and the aliphatic region were consistent with literature spectra.[32] Significant resonances are present around 2 ppm, indicating that the acetonitrile was not completely evaporated. The resonance at 2.2 ppm is attributed to acetone (likely because the NMR tube was not completely dry), and the resonance at 2.7 ppm is consistent with that of succinimide.

The characterization of the product of reaction 10 was also performed using LC-MS. Evaluation of the UV absorption, the Total Ion Current (TIC) and the mass fragmentation pattern. The chromatograms were recorded at three different wavelengths: 254 nm, 280 nm and 290 nm. These three chromatograms are shown below, in **Figure 2.7**.

UV set to 254 nm, **Figure 2.7a** includes a polar product. This wavelength is commonly used for general detection as most compounds have n-pi* transitions here, but it doesn't help in this case in providing detailed structural information. Histidine has a lambda-max at 211 nm.

In **Figure 2.7b**, UV is set at 280 nm. This comes close to the absorption maximum of histidine's imidazole side chain, which makes it more suitable for detecting similar compounds having similar structures.

At 311 nm, histidine has a weak absorption band, this means that the wavelength set to 290 nm, **Figure 2.7c**, could be diagnostic for the presence of a histidine structure.

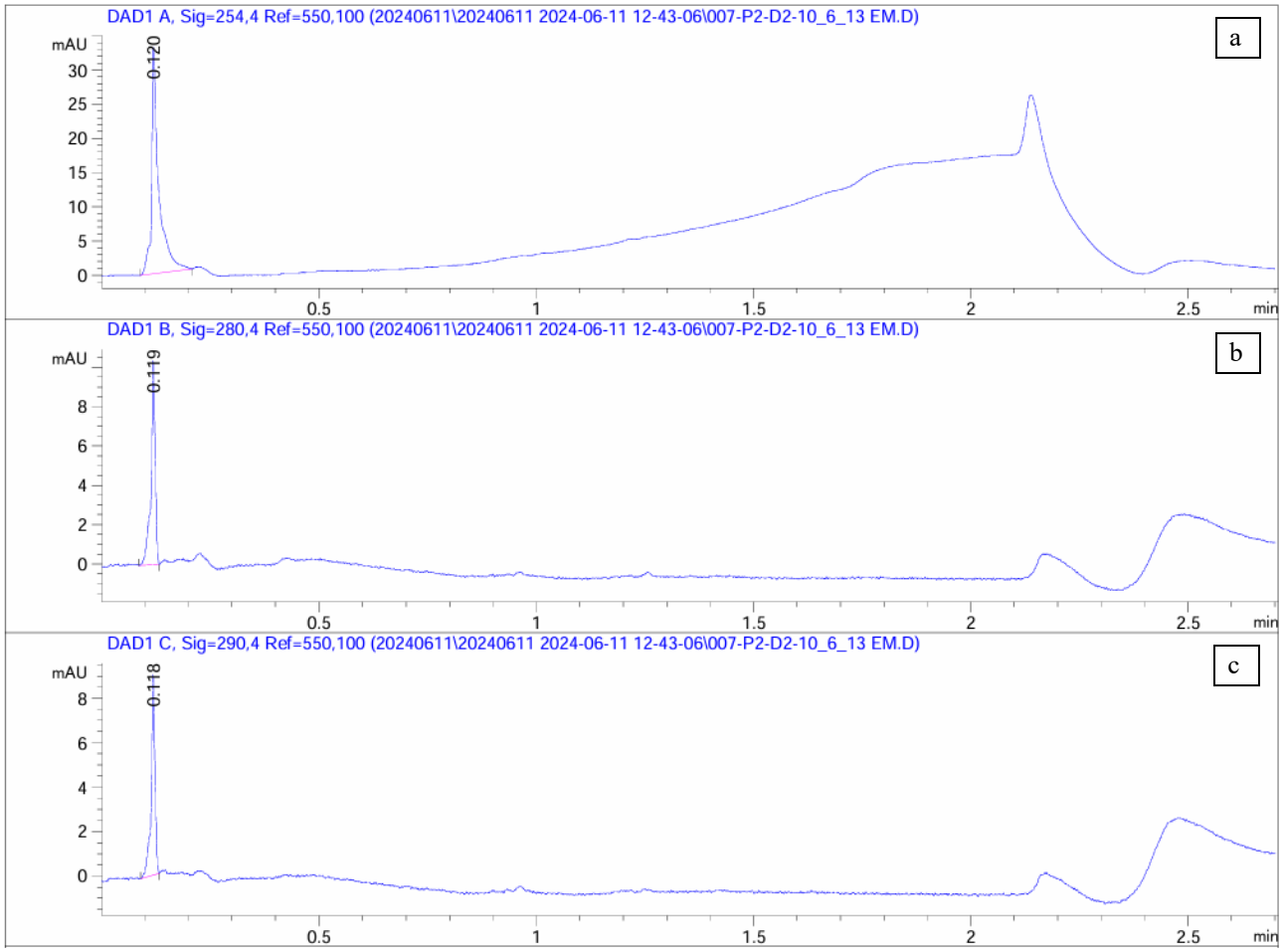

Figure 2.7. *UV-Vis spectra recorded at three different wavelengths: (a) 254 nm (b), 280 nm (c) 290 nm.*

The TIC chromatogram, shown in **Figure 2.8**, shows the ionisation peak at 0.139 min corresponding to the UV spectrum retention time of 0.118 min above (**Figure 2.7c**). This suggests that the compound detected is ionized in the mass spectrometer and is present in a significant amount.

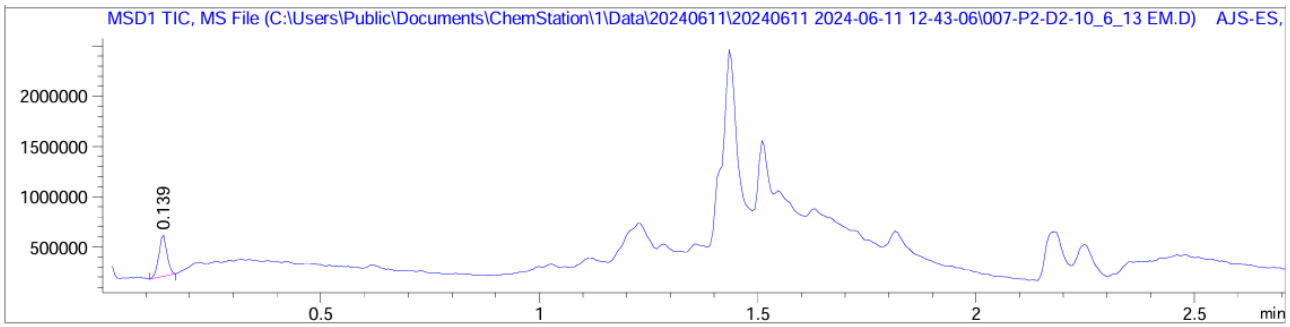

Figure 2.8. *Total Ion Current (TIC) analysis.*

The mass spectrum, **Figure 2.9**, corresponding to 0.139 min, shows several peaks. The fragment with a *m/z* ratio of 157 could be a common contaminant, which means it may not be related to the target compound. The fragment with *m/z* ratio of 198.2 could correspond to the loss of the *S*-acetyl group. The MS/MS spectrum of hercynine, as reported in the literature [38], identifies a molecular ion at *m/z* 198.1. The peak with a *m/z* ratio of 273.11 corresponds to **b**.

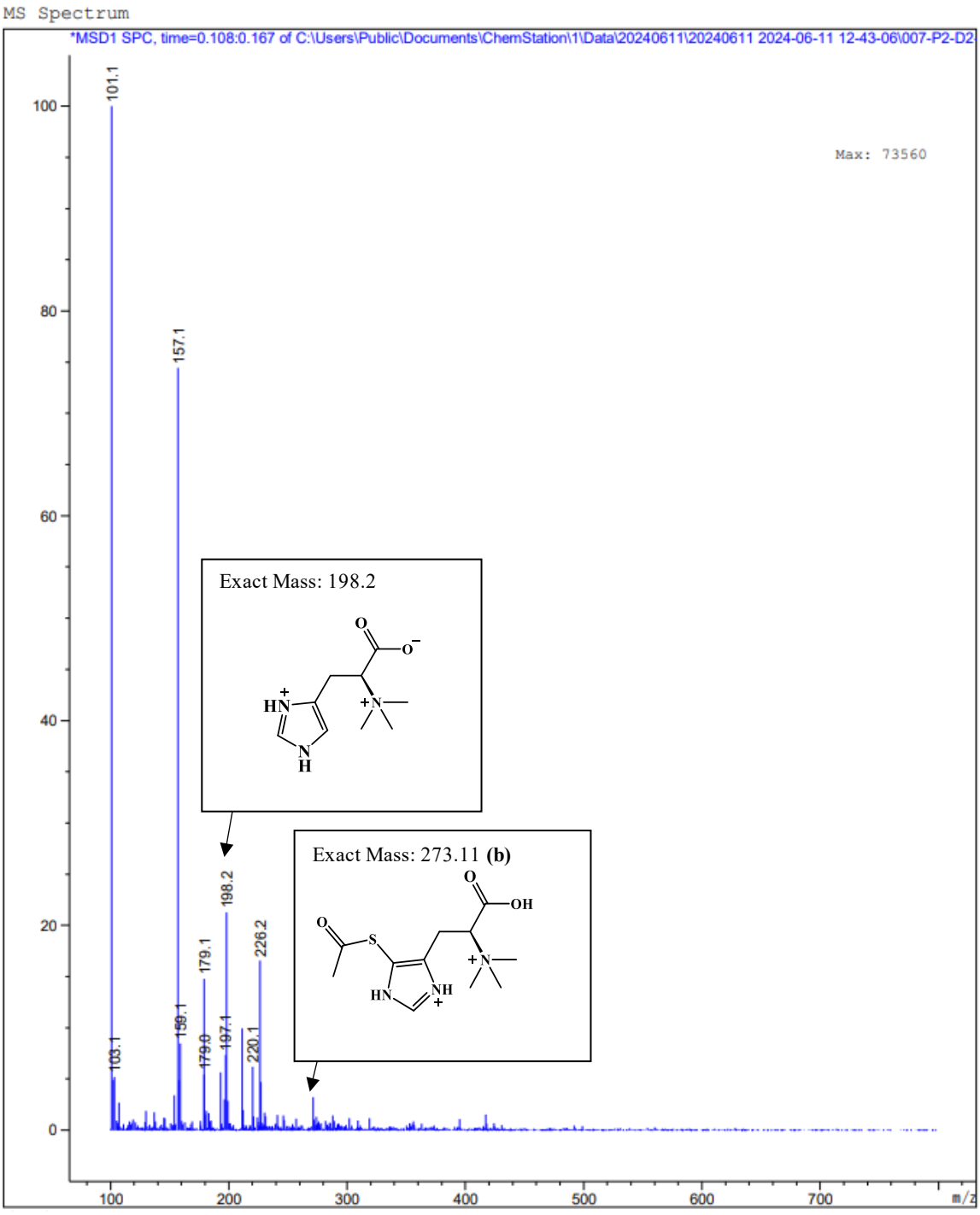

Figure 2.9. *MS Spectrum of reaction 10.*

As reactions 1-6, the quantities of reactants used were minimal, primarily to evaluate the behaviour on TLC and to obtain a sufficient amount of material for NMR and LCMS analysis. Therefore, the yield was not determined.

Motivated by the findings in reaction 10, reactions 12 and 13 were performed in the dark on a gram scale utilising thioacetic acid and cysteine as sulfur donors respectively. Despite the use of reversed-phase chromatography (C18) for purification, the resulting NMR spectra indicated persistent impurities, prompting an alternative purification approach.

Unlike the spectra obtained thus far, the NMR spectrum of reaction 12 exhibits a single peak in the aromatic region (**Figure 2.10**), suggesting a more selective or regio-specific transformation compared to previous reactions. The aliphatic region, on the other hand, remains consistent with the spectra analysed earlier, indicating the retention of key structural features.

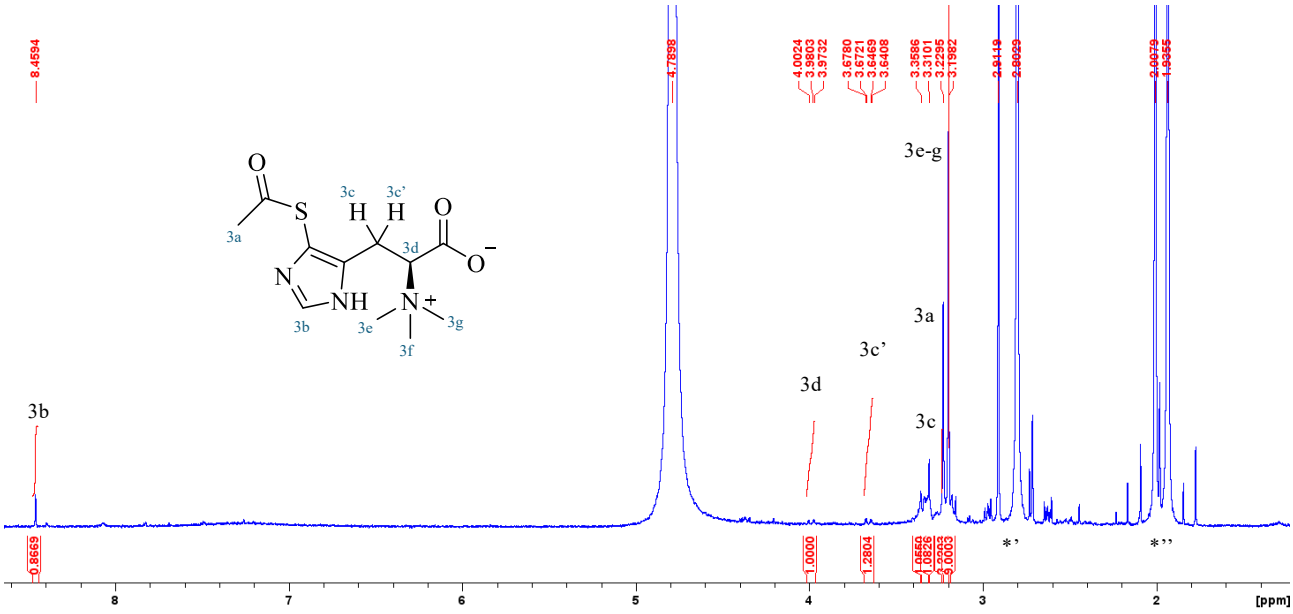

Figure 2.10. *NMR spectra of the product of reaction 12. D_2O is used as the solvent.*

**' traces of NBS and succinimide.*

**'' traces of residual acetonitrile, incomplete evaporation of acetone or traces of ethyl acetate (all of which were used at different stages of the reaction and purification process).*

After purification, 0.809 g of crude product was obtained for reaction 12. ^{1}H NMR analysis revealed the presence of a large amount of residual succinimide. By comparing the integration of the aromatic proton from the product (*3b*, ~1H) with the total succinimide signals (~250H), it was estimated that the product accounted for only ~0.398% of the crude mixture. This corresponds to an actual yield of 3.2 mg, or 0.30%, calculated against the theoretical maximum based on the starting hercynine.

Despite the extremely low yield, this result marks a qualitative improvement. In earlier reactions, the aromatic region of the NMR spectrum typically showed two signals, one of which was unassignable. In this case, only a single, well-defined aromatic peak was present, clearly attributable to the desired product. This represents a small but meaningful step forward in terms of selectivity and product identification, indicating that the optimized reaction and purification conditions, though not yet efficient, may be steering the outcome in the right direction.

In contrast, the NMR spectrum of reaction 13 (thiolation with cysteine) did not yield the thiolated product, as the characteristic signals of the desired product were absent. Due to poor solubility the reaction involving cysteine may require optimized conditions or prolonged reaction times to achieve complete conversion. Thiol-based substitutions often exhibit slower reaction rates compared to other nucleophiles as well as competing oxidation to the disulfide which may further explain the incomplete conversion observed in this case.

Solid-Liquid Purification (Reaction 14)

Reaction 14 sought to refine purification techniques further by employing solid-liquid extraction instead of chromatography (**Scheme 2.6**). Since the NMR spectrum related to reaction 13 did not show the desired signals, it was hypothesized that cysteine required a longer reaction time to complete the reaction.

For reaction 14, in which cysteine was again used as the sulfur donor, however, this time the reaction time of the second step was extended to 3 days as an attempt to improve the conversion.

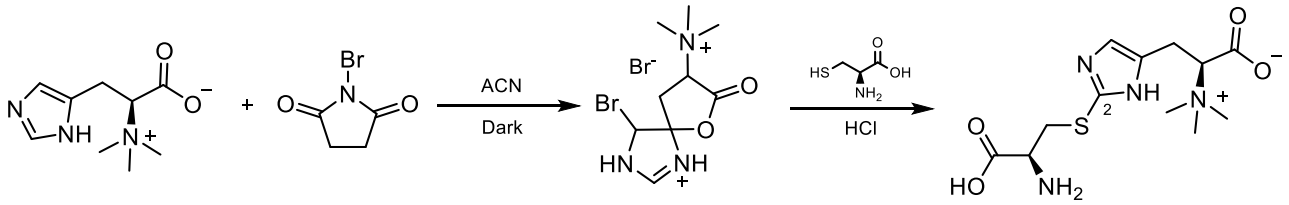

Scheme 2.6 (Reaction 14): *Synthesis of 3-{2-[(2-amino-2 carboxyethyl)thio]-1H-imidazol-4-yl}-2-(trimethylammonio) propanoate (cysteinylhercynine).*

Before initiating the second reaction step the reaction mixture was degassed using liquid nitrogen. Only after this procedure was cysteine introduced to commence the subsequent transformation.

The degassing step was performed to eliminate any oxygen that might be present in the reaction environment, as its presence could lead to the oxidation of cysteine, thus rendering it inactive as a nucleophile.

As a purification strategy, solid–liquid extraction was employed. After evaporation of solvents from reaction 14, ethyl acetate was first added to extract impurities. The residual solid product was then isolated, and was subsequently extracted with isopropanol, which is more polar than ethyl acetate. Finally, ethanol was used for the last extraction step. It was essential to quantify the amount of material dissolved in each solvent (**Table 2.4**).

Each extraction was monitored using thin-layer chromatography (TLC), with Gibbs reagent as a staining agent. Gibbs reagent (2,6-dichloroquinone-4-chloroimide) is often used in thin-layer chromatography to help detect compounds that contain imidazole groups. When applied to the TLC plates, it reacts with the imidazole ring to form a bright pink complex, making it easier to see and track the transformation of hercynine.[39]

The compound extracted in isopropanol, for the reaction 14, showed an intense yellow colour and was visible under UV light at 254 nm without additional staining.

However, it is expected that the material obtained with ethyl acetate and isopropanol consists mainly of impurities. It is possible that isopropanol also extracted a small amount of the target compound, but the amount remains relatively low. The final extraction was performed in ethanol, because this solvent can dissolve the target compound. Upon the addition of ethanol, some salt remained insoluble. The ethanol-soluble fraction from reaction 14 appeared light yellow. The extracted fractions led to significantly cleaner NMR spectra, confirming the effectiveness of this purification method.

Table 2.4. *Amount of compound dissolved in each solvent during the solid-liquid extraction.*

Reaction	***Thiolating agent***	***Amount of hercynine used***	***Fraction soluble in ethyl acetate***	***Fraction soluble in isopropanol***	***Fraction soluble in ethanol***
14	Cysteine	~2g	~7mg	~180mg	~1g

To further improve purification, a liquid-liquid extraction was introduced prior to a solid-liquid extraction (**Figure 2.11**).

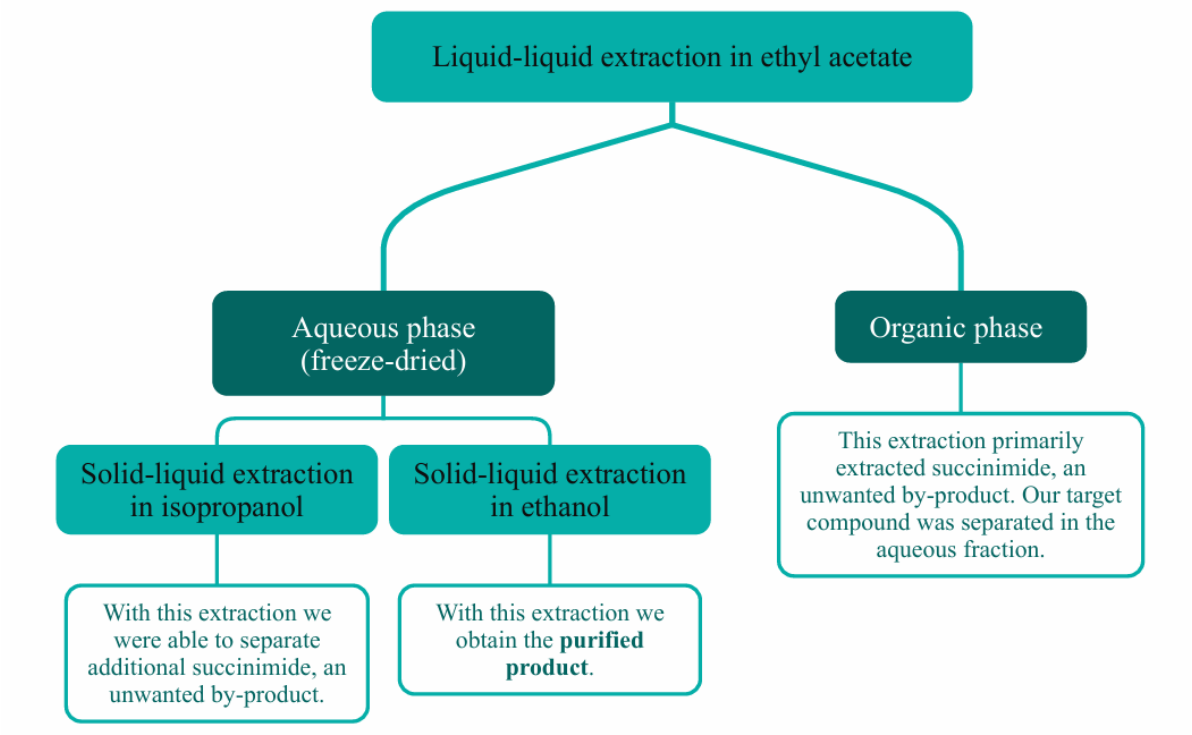

Figure 2.11*. Purification method applied to the cysteinylhercynine product (reaction 14).*

This purification approach yielded the cleanest NMR spectra (**Figure 2.12**) observed throughout the study, suggesting a significant reduction in impurities and improved structural integrity of the final compound.

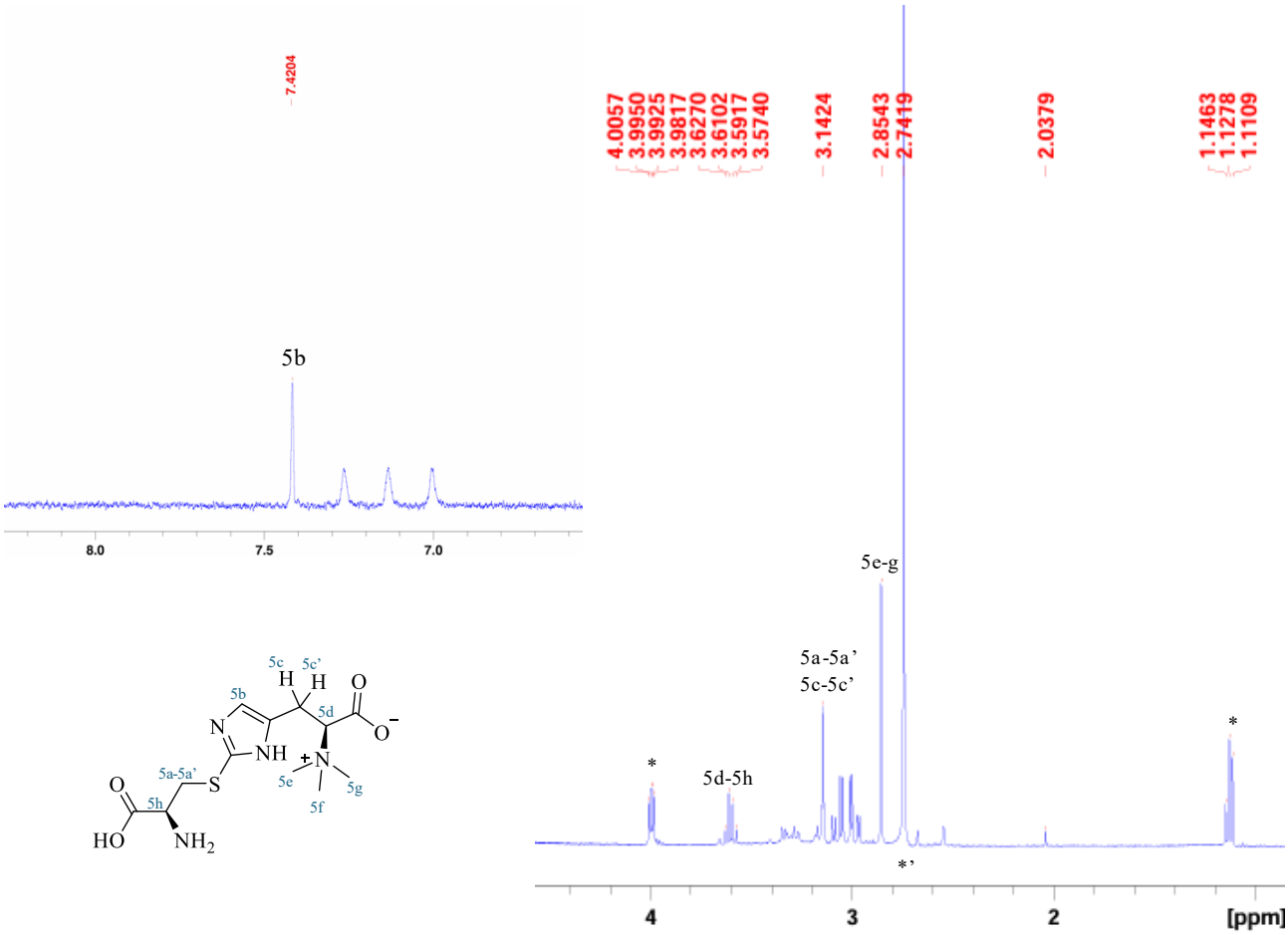

Figure 2.12. *NMR spectra of the product purified in ethanol from reaction 14. D_2O is used as the solvent.*

** trace of residual ethanol.*

**' trace of residual succinimide.*

The purification method employed in this reaction effectively removed a substantial portion of the succinimide byproduct, as well as other side products and unreacted reagents. Furthermore, no column chromatography was required for purification, which was a key objective of this project, considering the high costs and extended processing times associated with column-based purification.

The signal in the aromatic region at 7.42 ppm (**5b**) appears to be very weak. Additionally, broadened peaks are visible in the same region, indicative of NH_4Cl salt. The signals for ethanol and succinimide were also present.

The multiplet at approximately 3.6 ppm corresponds to an overlap of two signals: a more deshielded triplet, indicative of the CH bonded to the quaternary nitrogen (**5d**), and a more shielded double doublet, corresponding to the α-H (**5h**).

Around 3.14 ppm, a series of double doublets can be assigned to the CH_2 groups within the molecule. At higher ppm values, two double doublets correspond to a pair of protons from a -CH_2 group in a deshielded environment, such as the methylene between the thiol and carboxyl groups (**5a-5a'**).

At slightly lower ppm values, another set of double doublets corresponds to a second methylene group located in a slightly different environment (**5c-5c'**). Finally, a singlet at 2.85 ppm was assigned to the trimethylammonium group (**5e-g**).

Following the modified purification procedure based on sequential liquid–liquid and solid–liquid extractions, 0.5708 g of crude product was recovered from the ethanol-soluble fraction. The extraction sequence significantly reduced the amount of residual succinimide, and only minor traces were still detectable by ^1H NMR. Nonetheless, analysis of the aromatic region indicated that the product was present in a relatively low proportion within the crude mixture.

Despite the limited amount obtained, the spectrum clearly showed a distinct aromatic signal attributable to the target compound. This is an encouraging result, as previous experiments often resulted in more complex aromatic patterns or overlapping signals that hindered confident identification. The current outcome suggests an improvement in product selectivity and provides a solid basis for further optimization of the reaction and purification conditions.

Conclusion: Summary of Results and Future Perspectives

Overall, this progressive refinement of reaction conditions and purification techniques enabled the identification of an optimized synthetic pathway.

Following the extensive evaluation of reaction conditions, it became evident that achieving high selectivity and purity required not only an optimized synthetic approach but also an effective purification strategy. Even with improvements in reaction efficiency, the presence of residual reactants, by-products such as succinimide, and solvent traces necessitated a detailed investigation of purification techniques to obtain a chemically pure final product.

Initially, purification was attempted using a normal phase and a reversed-phase column chromatography (C18), a widely utilized method for separating organic compounds based on charge and hydrophobic interactions. While this approach provided partial separation of the desired compound from unwanted by-products, inconsistencies in product purity suggested the need for alternative strategies. The primary limitation observed in chromatography was the co-elution of structurally similar charged impurities, which hindered complete resolution of the product.

To address these challenges, solid-liquid extractions were systematically explored. This method exploits differences in solubility between the target compound and impurities across multiple solvents. The selection of appropriate solvents was guided by theoretical solubility parameters. Successive extractions with ethyl acetate, isopropanol, and ethanol enabled stepwise removal of residual reactants and undesired side-products. Ethyl acetate preferentially extracted non-polar impurities, while ethanol facilitated the recovery of the polar target compound, minimizing contamination.

Furthermore, the impact of freeze-drying as a final purification step was examined. This technique effectively removes residual solvent by sublimation under reduced pressure, preventing thermal degradation of heat-sensitive compounds.

The implementation of freeze-drying significantly improved the stability of the final product, as confirmed by NMR and LC-MS analyses.

The final purification process, integrating solid-liquid extraction and freeze-drying, yielded a product with spectral properties in agreement with literature references, confirming its structural integrity. These findings underscore the critical role of purification in organic synthesis and highlight the necessity of modifying post-reaction processing to the specific physicochemical properties of the target compound.

Particular attention was also given to the choice of solvent, as it plays a crucial role in reaction efficiency and sustainability. Acetonitrile was initially tested as a complete replacement for aqueous HCl; however, its limited ability to fully dissolve hercynine necessitated a modification in the reaction strategy. To address this issue, acetonitrile was used exclusively in the first step, while aqueous HCl was introduced in the second step to enhance reagent solubility.

One of the key advantages of acetonitrile in this approach was its easy removal via rotary evaporation, something that would not have been feasible with higher-boiling-point alternatives. Despite the use of a different solvent in the first step, careful purification allowed the isolation of a final product with an NMR spectrum comparable to literature data. These findings confirm that, although aqueous HCl remains essential for the second step, a mixed-solvent approach can be effectively implemented without compromising product integrity.

This study underscores the importance of solvent selection in organic synthesis, demonstrating that balancing solubility, volatility, and reactivity is crucial for optimizing reaction conditions. While aqueous HCl remains the conventional choice, the selective use of acetonitrile in the initial step presents a viable alternative that reduces exposure to strong acids, improving both safety and environmental impact.

Determination of Ergothioneine Antioxidant Properties

Introduction

Determination of antioxidant strength using the ABTS decolorization assay

The ABTS decolorization assay is a widely used spectrophotometric technique designed to evaluate the total antioxidant capacity and the antioxidant activity of various compounds.[40,41] This method employs Trolox, a water-soluble derivative of vitamin E, as a reference antioxidant. The assay is frequently referred to as the Trolox Equivalent Antioxidant Capacity (TEAC) assay, as the results are typically expressed in terms of Trolox equivalents (TE). It is also known as an electron transfer (ET) assay, as it quantifies an antioxidant's ability to transfer electrons, thereby reducing an oxidizing agent and inducing a colour change.[42]

TE or TEAC values provide a standardized means of comparing the antioxidant potency of different substances, considering the concentration or volume of the antioxidant being tested.[43] This assay is versatile, capable of assessing a broad spectrum of antioxidants, both hydrophilic and lipophilic, due to the solubility of ABTS in both aqueous and organic solvents. Moreover, the assay is adaptable to a wide pH range, which enhances its applicability across various experimental conditions.[43,44]

The mechanism underlying the ABTS decolorization assay involves the reaction between an antioxidant and the $ABTS^{\bullet+}$ radical cation. The $ABTS^{\bullet+}$ radical can be generated through two different methods. A less common approach involves the use of hydrogen peroxide to oxidize ABTS into $ABTS^{\bullet+}$, catalysed by myoglobin in a pseudo-peroxidase reaction.[45] However, the more widely adopted method relies on potassium persulfate (or sodium persulfate), which reacts with ABTS in sub-stoichiometric amounts to generate the radical, as illustrated in **Scheme 3.1**.[43] This reaction requires a minimum of 12 hours to reach completion before the assay can be performed.

This reaction forms the basis for the assay's colorimetric measurements, as the antioxidant's ability to neutralize the radical results in a decrease in colour intensity, which is monitored spectrophotometrically. This modified procedure, often referred to as the "improved ABTS radical cation decolorization assay", is simpler, more cost-effective, and requires less specialized equipment, making it the method of choice for this study.[43,46]

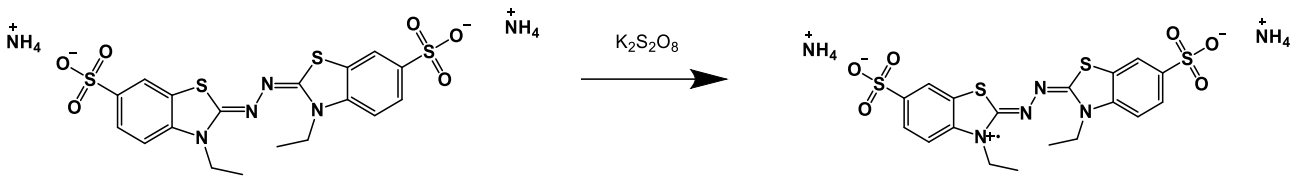

Scheme 3.1. *Oxidation of ABTS to ABTS$^{\bullet+}$ using potassium persulfate.*[43]

ABTS undergoes a stoichiometric reaction with potassium persulfate in a 1:0.5 ratio. However, this leads to incomplete oxidation upon the initial mixing, necessitating an incubation period of at least 12 hours.[46] The formation of the ABTS$^{\bullet+}$ radical is indicated by the development of a dark blue/green colour.

This radical exhibit absorption maxima at wavelengths of 414-417, 645, 734, and 815 nm. For most antioxidant capacity assays, the measurement is typically performed at 734 nm (**Figure 3.1**), as this wavelength minimizes interference from plant pigments.[42,47]

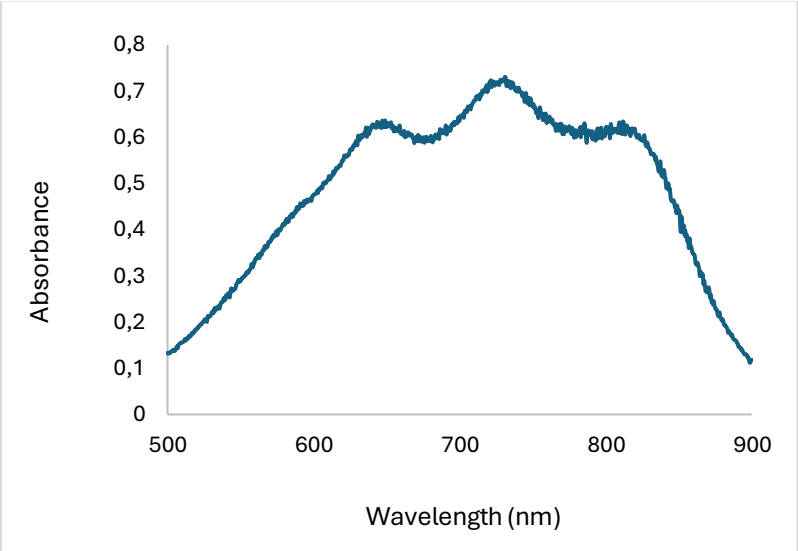

Figure 3.1. *UV-Vis spectra of ABTS$^{\bullet+}$ showing the maximum absorbance at 645, 734 and 815 nm.*

The reduction of the ABTS$^{\bullet+}$ radical occurs when it interacts with an antioxidant, leading to a transformation of the radical cation back to the neutral ABTS form. This reduction is accompanied by a colour change from blue/green to a lighter blue/green or colourless.

The decolorization process is attributed to the quenching of the ABTS$^{\bullet+}$ radical's hydrogen atom by hydrogen-donating antioxidants.[48] This reaction is influenced by both the antioxidant's concentration and its activity, as well as the duration of the interaction. Typically, antioxidant activity is measured 4-6 minutes after the initial interaction between ABTS$^{\bullet+}$ and the antioxidant.

Absorbance readings are then used to assess the change in ABTS$^{\bullet+}$ concentration.[43] The extent of decolorization can be expressed as a percentage of inhibition and plotted against concentration, with results often compared to the reactivity of Trolox.[46]

The ABTS$^{\bullet+}$ radical is neutralized through a single electron transfer (SET) mechanism.[49] When Trolox interacts with the ABTS$^{\bullet+}$ radical, the reaction occurs in two steps, as outlined in **Scheme 3.2**. In this scheme, Trolox-OH, Trolox-O, and Trolox=O represent Trolox-phenol, the Trolox semiquinone radical, and Trolox quinone, respectively.

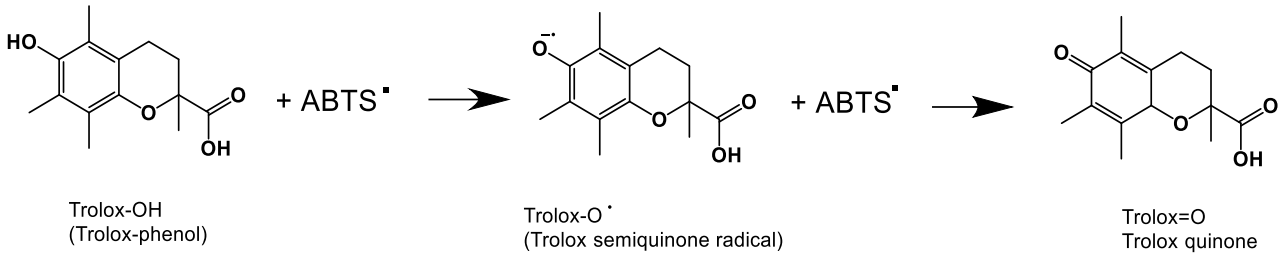

Scheme 3.2. *Reaction of ABTS•+ with Trolox.*[43]

$$\mathrm{ABTS}^{\cdot} + Trolox - OH \rightarrow ABTS + Trolox - O^{\cdot} + H^{+} \quad (1)$$

$$\mathrm{ABTS}^{\cdot} + Trolox - O^{\cdot} \rightarrow ABTS + Trolox = O \quad (2)^{43}$$

Results and Discussion

ABTS Decolorization Assay

The ABTS decolorization assay[46] was employed to evaluate the antioxidant capacity of various compounds, including L-(+)-ergothioneine, cysteine, and penicillamine, using Trolox as a reference standard.[50,51] The selection of Trolox as a standard is attributed to its stability, solubility in both aqueous and organic solvents, and well-characterized reactivity with the $ABTS^{\bullet+}$ radical cation. For each antioxidant, solutions were prepared at concentrations ranging from 50 to 400 μM, while Trolox standards were prepared in the range of 25 to 400 μM. The $ABTS^{\bullet+}$ solution, adjusted to an absorbance of 0.7 at 734 nm, was added to each antioxidant in a ratio of 20:1 $ABTS^{\bullet+}$ to antioxidant. The resulting mixtures were equilibrated at 30°C for 6 minutes, after which their UV-Vis spectra were recorded over a wavelength range of 500–900 nm. All tested antioxidants exhibited a significant capacity to scavenge the $ABTS^{\bullet+}$ radical cation, leading to visible colour changes, from dark blue to colourless. The ability of these compounds to scavenge $ABTS^{\bullet+}$ is attributed to their electron-donating properties, which facilitate the reduction of the radical cation, leading to a decrease in absorbance at 734 nm. Trolox serves as a standard due to its well-characterized antioxidant capacity, allowing for the quantification of radical scavenging efficiency in TEAC values. Similarly, cysteine and penicillamine exhibit strong reducing potential, while L-(+)-ergothioneine demonstrates significant radical-quenching activity due to its resonance-stabilized structure. **Figures 3.2** to **3.5**, shown below, illustrate the UV-Vis spectra representing the radical scavenging abilities of Trolox, cysteine, penicillamine, and L-(+)-ergothioneine, demonstrating the quenching of the $ABTS^{\bullet+}$ radical cation at different antioxidant concentrations. The degree of decolorization caused by each antioxidant was measured and expressed as a percentage inhibition. Each data point represents the average of three trials, with absorbance measured three times for each trial. The standard curves of inhibition (%) versus concentration (μM) for each antioxidant are presented in **Figures 3.6** to **3.9**.

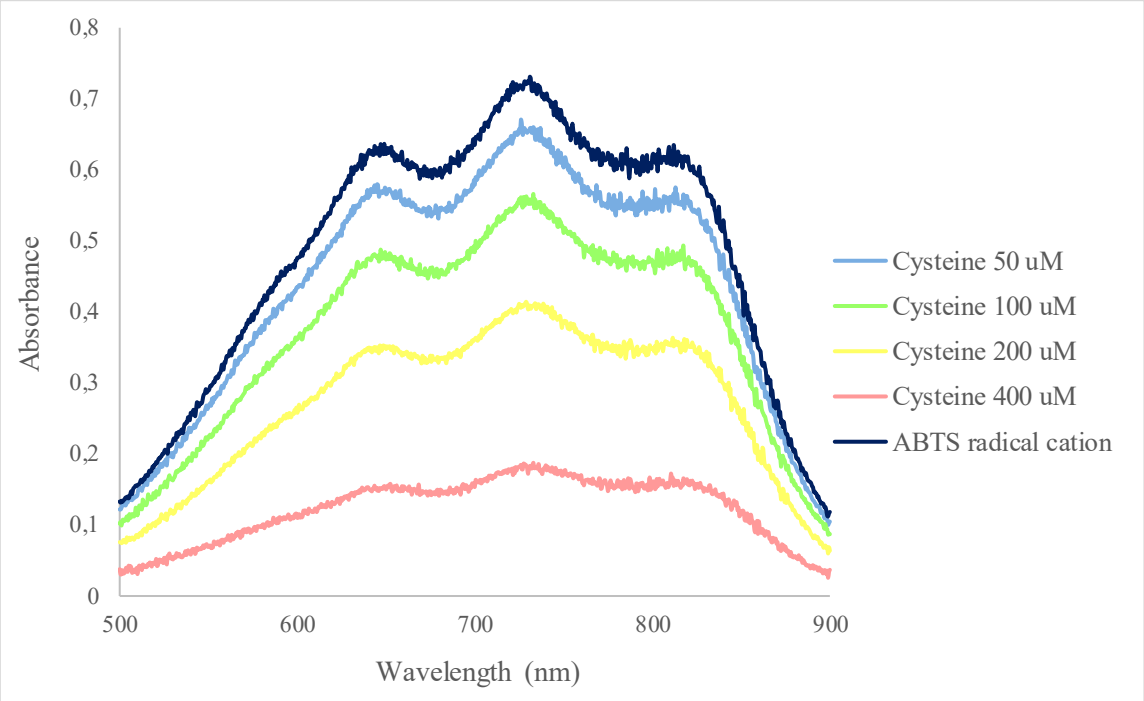

***Figure 3.2**. UV-Vis spectra showing quenching of ABTS$^{\bullet+}$ by cysteine, at different concentrations (µM).*

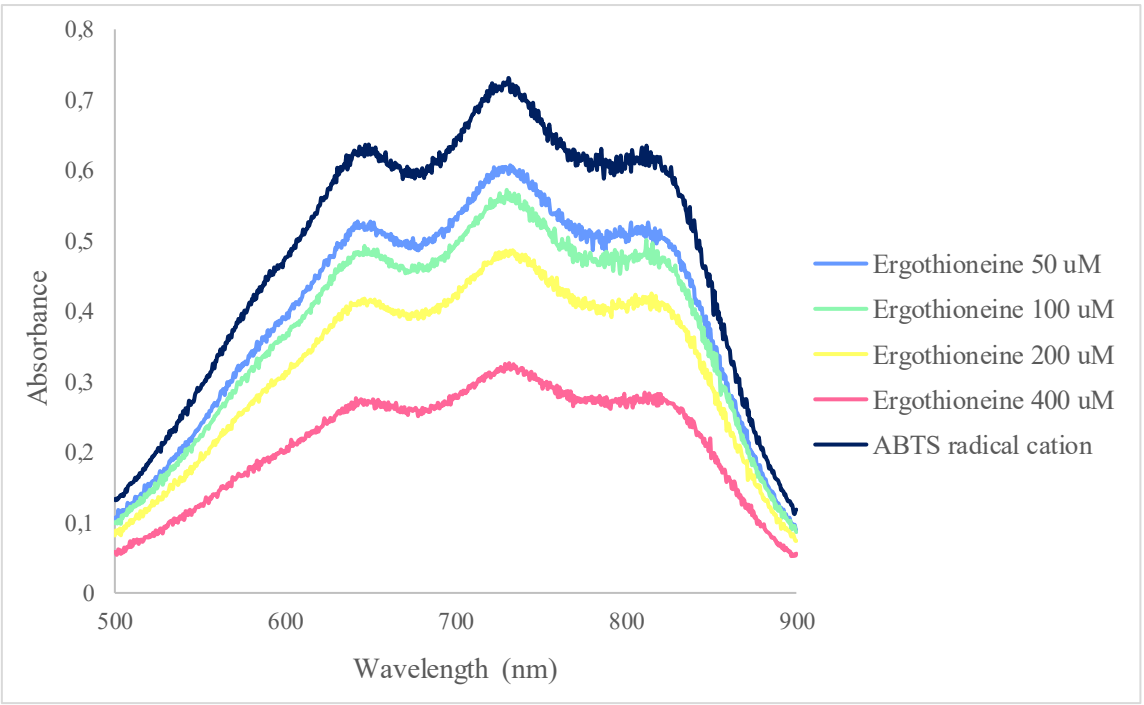

***Figure 3.3.** UV-Vis spectra showing quenching of ABTS$^{\bullet+}$ by L-(+)-ergothioneine, at different concentrations (µM).*

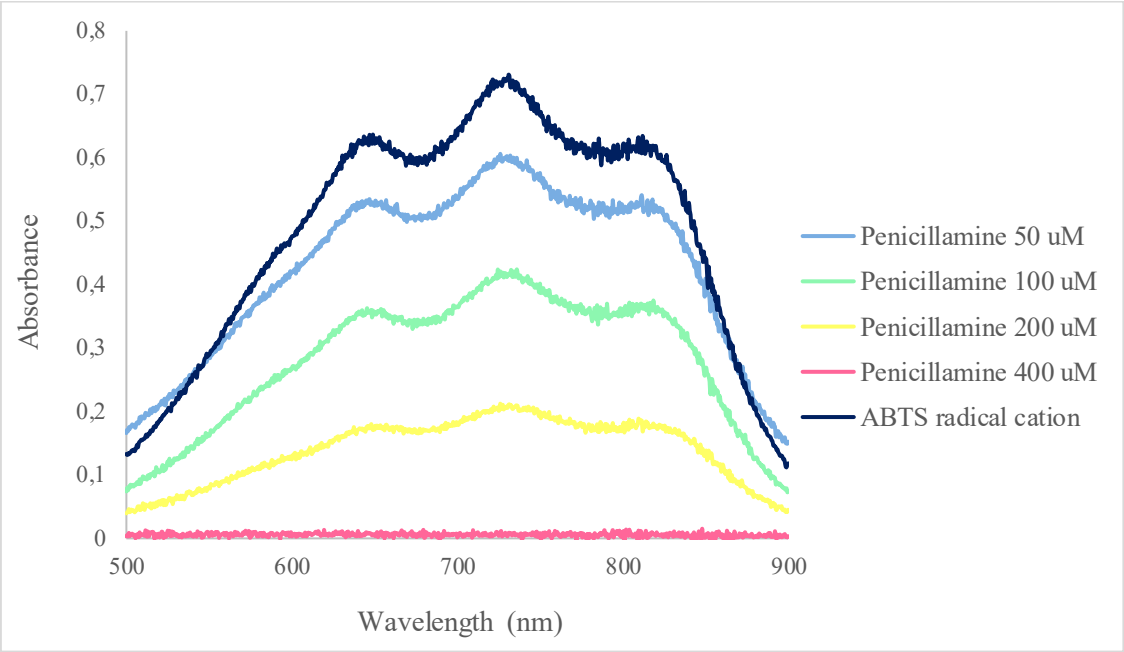

Figure 3.4. *UV-Vis spectra showing quenching of ABTS$^{\bullet+}$ by penicillamine, at different concentrations (μM).*

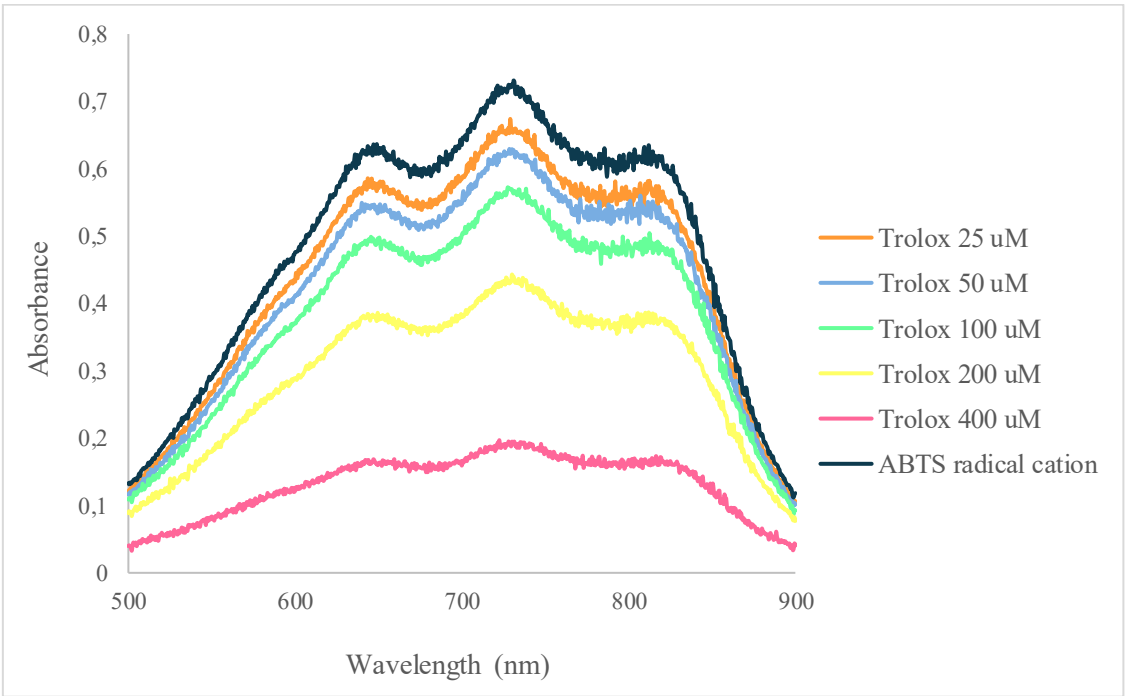

Figure 3.5. *UV-Vis spectra showing quenching of ABTS$^{\bullet+}$ by Trolox, at different concentrations (μM).*

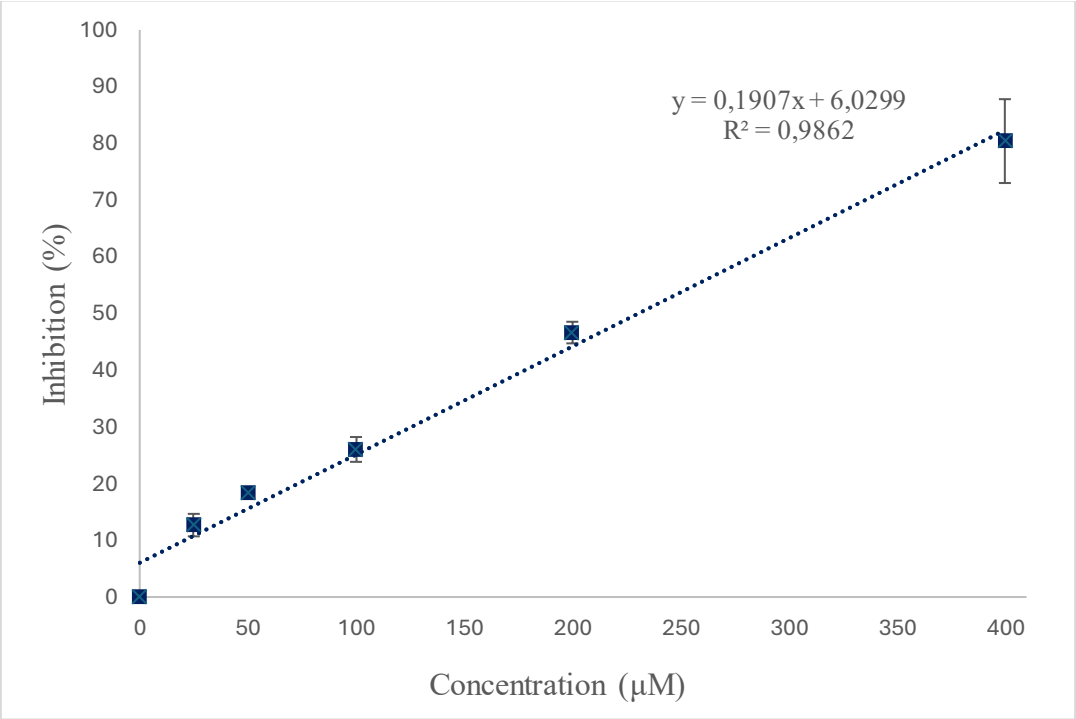

Figure 3.6. *Standard curve representing the average inhibition (%) displayed by Trolox at a range of concentrations (µM). Absorbance values measured at 734 nm. Error bars show the standard deviation in the inhibition (%); n = 3.*

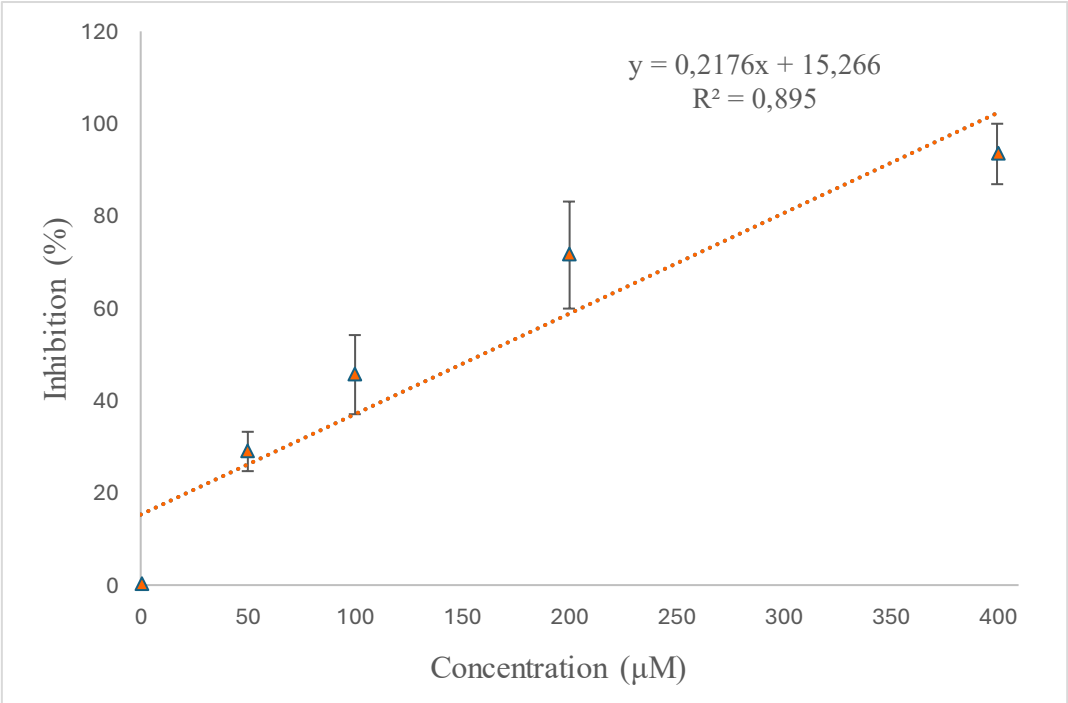

Figure 3.7. *Standard curve representing the average inhibition (%) displayed by penicillamine at a range of concentrations (µM). Absorbance values measured at 734 nm. Error bars show the standard deviation in the inhibition (%); n = 3.*

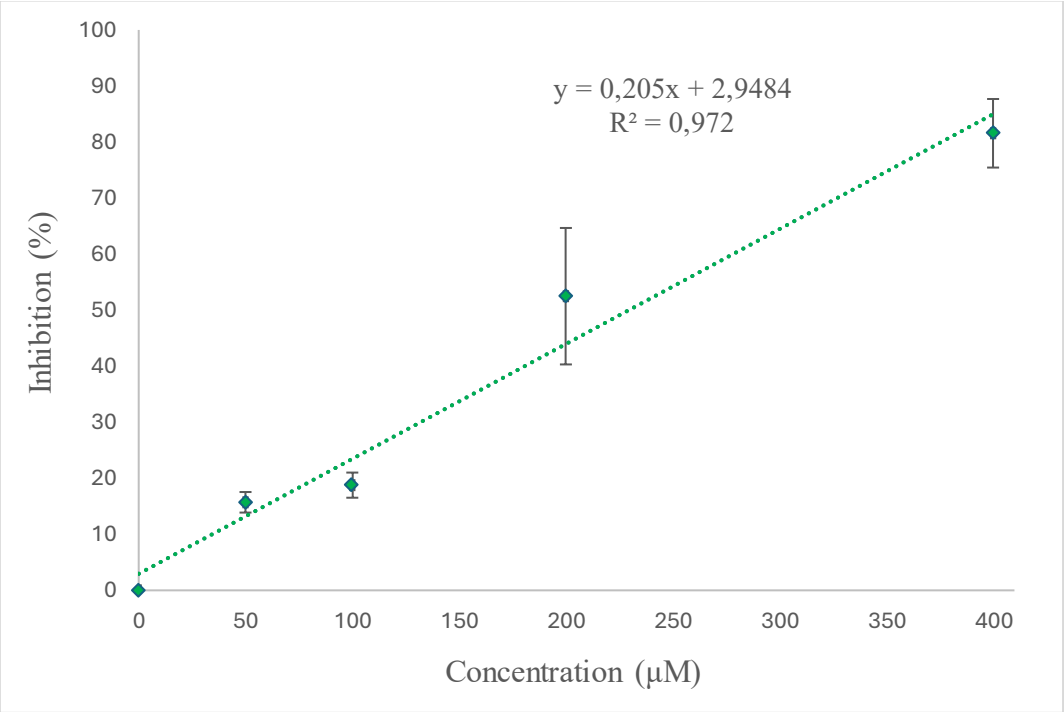

Figure 3.8. *Standard curve representing the average inhibition (%) displayed by cysteine at a range of concentrations (µM). Absorbance values measured at 734 nm. Error bars show the standard deviation in the inhibition (%); n = 3.*

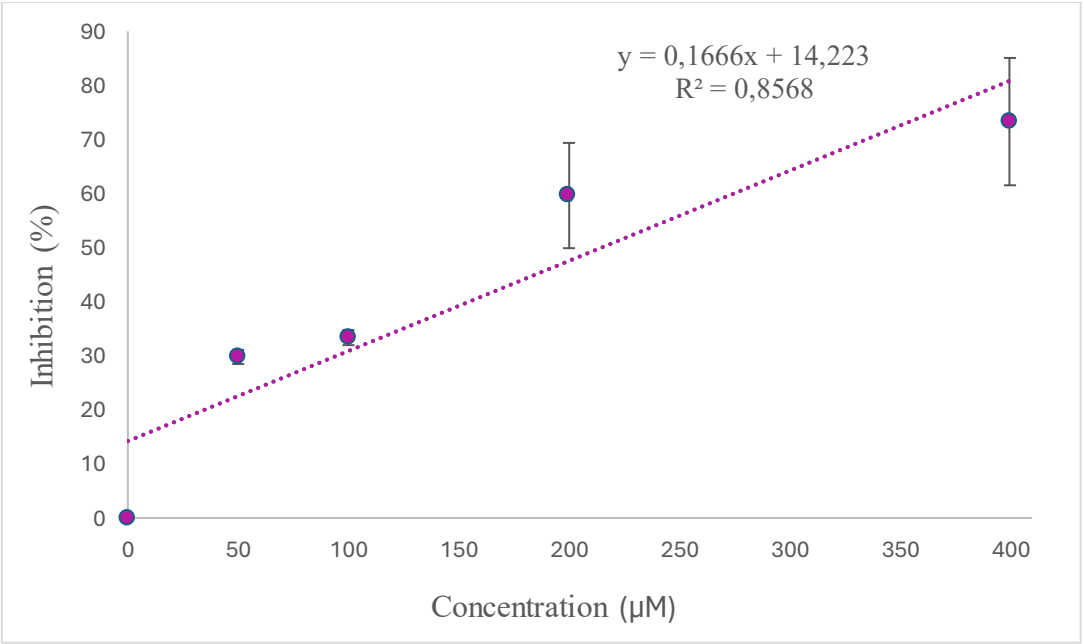

Figure 3.9. *Standard curve representing the average inhibition (%) displayed by L-(+)-ergothioneine at a range of concentrations (µM). Absorbance values measured at 734 nm. Error bars show the standard deviation in the inhibition (%); n = 3.*

Figure 3.10 represents the inhibition (%) resulting from each antioxidant at a range of 0-400 µM. The antioxidant capacity of each compound relative to that of Trolox can be viewed.

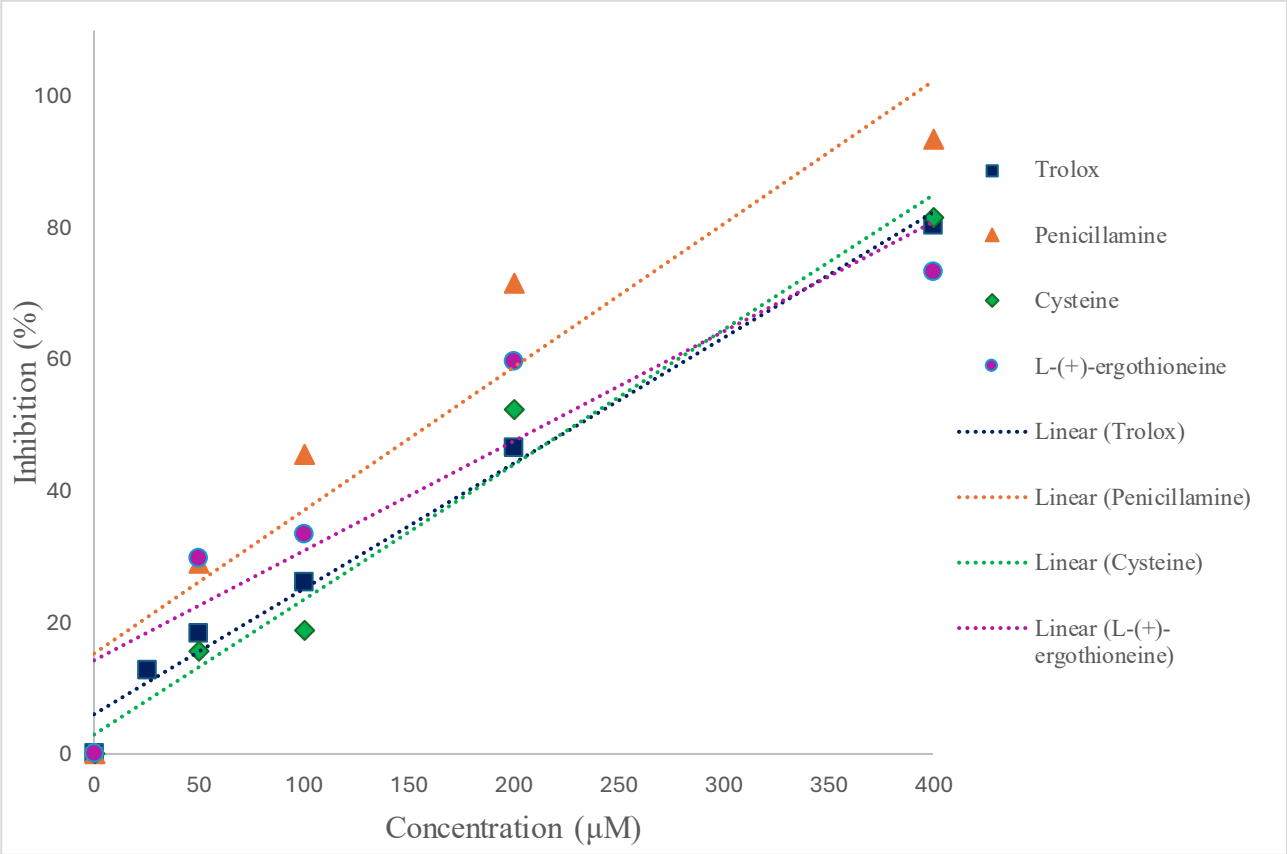

Figure 3.10. *TEAC value graphs showing the relative antioxidant capacity of cysteine, penicillamine and L-(+)-ergothioneine compared to Trolox.*

As previously mentioned, the Trolox Equivalent Antioxidant Capacity (TEAC) assay is a widely used method to evaluate the antioxidant capacity of various compounds by comparing their ability to scavenge the $ABTS^{\bullet+}$ radical cation relative to Trolox. In this assay, the TEAC value of each compound is determined by calculating the ratio of the slope (gradient) of the dose-response curve of the antioxidant to that of Trolox. This approach provides a standardized metric for assessing and comparing the antioxidant efficacy of different substances.[46]

The TEAC values obtained for each compound are presented in **Table 3.1**. These values facilitate a direct comparison of each antioxidant's capacity relative to Trolox.

Table 3.1. *TEAC values of several antioxidants were measured using the gradients of their standard curves. Standard deviation shown; n = 3.*

Compound	***TEAC value***
Trolox	1.00 ± 0.02
L-(+)-ergothioneine	0.874 ± 0.03
Penicillamine	1.14 ± 0.09
Cysteine	1.07 ± 0.04

The TEAC assay provides a standardized method for quantifying antioxidant strength by comparing the ability of different compounds to scavenge the $ABTS^{\bullet+}$ radical cation relative to Trolox. This approach facilitates the identification and characterization of potent antioxidants for potential therapeutic or nutritional applications. The method is widely used due to its simplicity, reproducibility, and capacity to evaluate both hydrophilic and lipophilic antioxidants, making it a valuable tool in antioxidant research and quality control within the food and pharmaceutical industries.

In this study, all analysed compounds demonstrated antioxidant properties, effectively scavenging the $ABTS^{\bullet+}$ radical cation. Both cysteine and penicillamine exhibited TEAC values close to 1, indicating antioxidant capacities comparable to Trolox. L-(+)-Ergothioneine, with a TEAC value of 0.874, also showed significant radical scavenging ability, albeit slightly lower than that of Trolox. Although slightly lower in this assay, previous studies, such as Franzoni et al. (2006)[52], using the TOSC method, have reported comparable antioxidant activity between ergothioneine and Trolox. Notably, if the analysis is restricted to concentrations up to 200 µM, the linear fit of the dose–response curve improves and EGT appears even more similar in efficacy to Trolox.

These findings highlight the potential of these compounds as antioxidants, with varying degrees of efficiency in neutralizing free radicals.

Conclusion: Summary of Results and Future Perspectives

ABTS decolorization assay

The $ABTS^{\bullet+}$ decolorization assay is, as already known, a well-established method for evaluating the antioxidant capacity of various compounds by measuring their ability to scavenge the $ABTS^{\bullet+}$ radical cation. This method provides a reliable comparison of antioxidant efficiency, specifically when using Trolox as a reference standard.[54]

In this study, the antioxidant properties of L-(+)-ergothioneine, cysteine, and penicillamine were measured based on their ability to neutralize the $ABTS^{\bullet+}$ radical cation. The results indicate that both cysteine and penicillamine exhibit scavenging capacities comparable to Trolox, with TEAC values close to 1. This suggests that these two compounds are nearly as effective as Trolox in reducing oxidative species within the system, meaning that their ability to donate electrons or hydrogen atoms to neutralize the $ABTS^{\bullet+}$ radical cation is comparable to that of Trolox. Since the TEAC value is derived from the ratio of the scavenging efficiency of a given compound relative to Trolox, a value close to 1 indicates that cysteine and penicillamine exhibit a similar reactivity towards the $ABTS^{\bullet+}$ radical. This implies that these compounds could serve as effective antioxidants in systems where Trolox is typically used as a reference or standard antioxidant. Their comparable efficiency suggests they may provide similar protective effects against oxidative damage in biological or industrial applications, such as in food preservation, pharmaceuticals, or cosmetic formulations designed to mitigate oxidative stress.

L-(+)-Ergothioneine displayed significant antioxidant activity, with a TEAC value of 0.874, indicating an effective ability to quench the $ABTS^{\bullet+}$ radical cation. Although this value appears slightly lower than that of Trolox when considering the full concentration range tested, a re-analysis limited to concentrations up to 200 μM improves the linearity (R^2 value) of the dose–response curve.

Under these conditions, ergothioneine's antioxidant capacity becomes more comparable to that of Trolox, aligning more closely with previous findings in the literature.[52] Moreover, the biological relevance of L-(+)-ergothioneine as an antioxidant extends beyond the parameters of this specific assay, reflecting its known physiological roles in oxidative stress protection.

Unlike Trolox, which is a synthetic analogue of vitamin E primarily used as a reference compound in antioxidant studies, ergothioneine is a naturally occurring thiol compound that has been shown to accumulate in various tissues, including the liver, kidneys, eyes, and red blood cells.

This selective accumulation suggests that the body actively transports ergothioneine into cells via the OCTN1 transporter and retains it, highlighting its potential biological importance.

Moreover, ergothioneine has been recognized for its ability to mitigate oxidative stress in vivo, where it plays a role in protecting cells from reactive oxygen and nitrogen species. Its unique stability, resistance to auto-oxidation, and ability to regenerate after scavenging free radicals distinguish it from other antioxidants that may degrade more rapidly. Additionally, recent research has linked ergothioneine to potential protective effects against neurodegenerative diseases, cardiovascular conditions, and inflammatory disorders, further emphasizing its physiological relevance. Therefore, while the TEAC value derived from the $ABTS^{\bullet+}$ decolorization assay suggests a slightly lower radical scavenging efficiency compared to Trolox, this does not reduce the broader significance of ergothioneine as a biologically relevant antioxidant. Its role in cellular protection, particularly in tissues prone to oxidative damage, supports its importance in human health and its potential application in dietary supplements, medical nutrition, and therapeutic formulations.

Overall, these findings highlight the varying degrees of antioxidant capacity among the tested compounds, emphasizing their potential applications in biological and pharmaceutical contexts.

The strong scavenging abilities of cysteine and penicillamine support their role as effective antioxidants, while L-(+)-ergothioneine remains an important molecule due to its known physiological functions despite its slightly lower efficiency in the $ABTS^{\bullet+}$ assay.

Experimental

Materials and Methods

Reagents were purchased from commercial sources (Sigma-Aldrich, Merck, Fluorochem, Roche). Solvents were obtained from Sigma-Aldrich or Merck. Aqueous solutions were prepared using deionised water. Solutions and buffers used for the ABTS decolorization assay were prepared using Milli-Q water.

Thin Layer Chromatography (TLC) analysis was used to monitor reaction progression using Sigma-Aldrich silica gel 60 F254 plates, and Gibbs reagent dissolved in ethanol was used to visualise compounds.

Aqueous compounds were lyophilized using a Virtis Benchtop K freeze-dryer. Ultraviolet-visible (UV-Vis) spectrometry was carried out using an Agilent Technologies Cary 60 UV-Vis spectrophotometer. UV-Vis spectra were recorded at wavelengths ranging from 500-900 nm, and absorbance measurements were measured at 734 nm. Organic solvents were removed from solution using the Buchi Vacuum Controller V-850 Rotovap. Solutions were purified through chromatography using silica gel.

^{1}H NMR were recorded on Bruker 400 MHz. Chemical shifts (δ) are reported in units of ppm. ^{1}H NMR spectra were recorded at 400 MHz using D_2O (4.79 ppm) solvents.

LCMS analyses were carried out with a UHPLC Agilent 1290 Infinity Series (Germany), accurate mass spectrometer Agilent 6530 Qradrupole Time Of Flight (QTOF) equipped with an Agilent jet stream ionization source (positive ionization mode) (ESI+) and column (Eclipse + C18 RRHD 1.8 µm.2.1 X 50, Agilent, Germany).

General Procedure of the synthesis

General procedure A: reactions 1 to 4

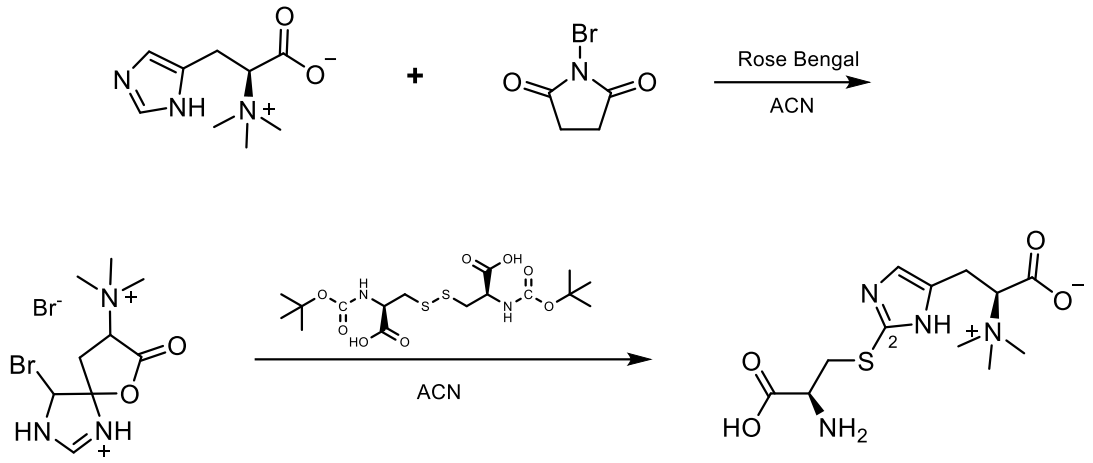

Reactions 1 and 3: *Synthesis of 3-{2-[(2-amino-2 carboxyethyl)thio]-1H-imidazol-4-yl}-2-(trimethylammonio) propanoate.*

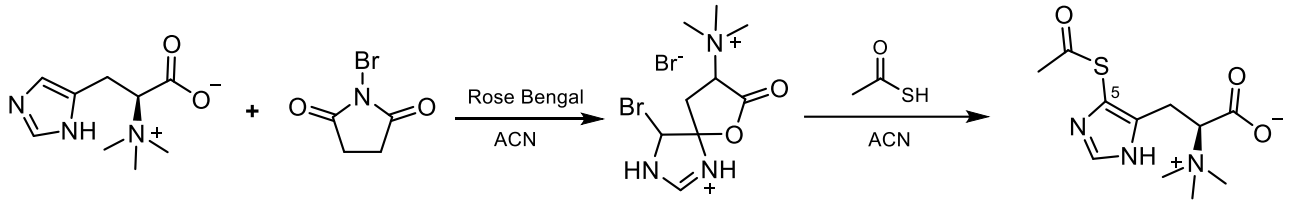

Reactions 2 and 4: *Synthesis of L-5-Acetylsulfanyl-αN,N,N-trimethyl-histidine.*

Acetonitrile (1 mL, 0.786 g) was added to L-hercynine (49.31 mg, 0.25 mmol, 1 equiv.) in a reaction vial. The mixture was stirred vigorously for several minutes. Subsequently, *N*-bromosuccinimide (NBS, 48.95 mg, 0.275 mmol, 1.1 equiv.) and Rose Bengal (2.62 mg, 0.0025 mmol, 0.01 equiv.) were added to the vial. Reactions 1 and 2 were placed inside the photoreactor at λ = 495 nm, while reactions 3 and 4 were placed inside the photoreactor at λ = 450 nm. The bromination step was carried out under continuous irradiation for 20 minutes. After this period, N-Boc-protected cystine (110.13 mg, 0.25 mmol, 1 equiv.) was added to reaction vials 1 and 3, while thioacetic acid (200 µL, 2.8 mmol) was added to reaction vials 2 and 4. The reaction mixtures were then left to react overnight under the respective irradiation conditions.

The reaction progress was monitored via Thin Layer Chromatography (TLC). The results showed that the profiles of reactions 2 and 4 were identical. Consequently, Sample 2 was combined with Sample 4, and the mixture was subjected to column chromatography using normal-phase silica gel and ethanol as elution solvent. To further purify the product, an additional elution was performed using a mixture of ethyl acetate, ethanol, and water (2 mL of water, 13 mL of ethanol, and 5 mL of ethyl acetate). As this was the first attempt, the quantities of reactants used were minimal, primarily to evaluate the behaviour on TLC and to obtain a sufficient amount of material for NMR analysis. Therefore, the yield was not determined.

General procedure B: reactions 5 and 6

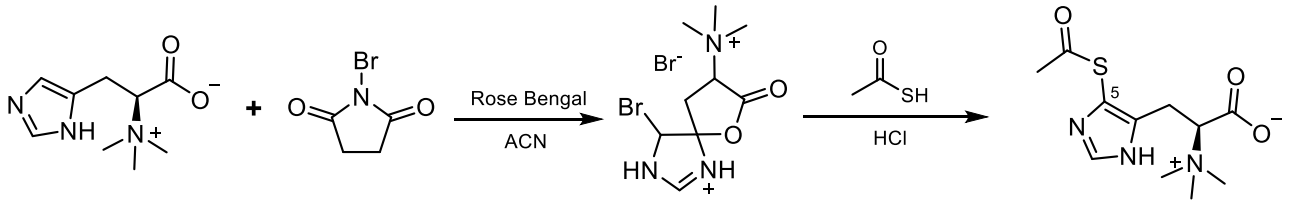

Reactions 5 and 6: *Synthesis of L-5-Acetylsulfanyl-α-N,N,N-trimethyl-histidine.*

Acetonitrile (2 mL, 1.572 g) was added to L-hercynine (98.62 mg, 0.50 mmol, 1 equiv.) in a reaction vial. The mixture was stirred vigorously for several minutes. Subsequently, *N*-bromosuccinimide (NBS, 97.90 mg, 0.55 mmol, 1.1 equiv.) and Rose Bengal (5.24 mg, 0.0050 mmol, 0.01 equiv.) were added to the vial. The reactions were still carried out under a 495 nm light source. In contrast to previous reactions, in reactions 5 and 6, after the bromination step (reaction time: 1 hour for reaction 5, overnight for reaction 6) acetonitrile was removed under reduced pressure using a rotary evaporator. The residue was then dissolved in an aqueous HCl solution (164 µL of HCl in 2 mL of water), followed by the addition of thioacetic acid (400 µL, 5.5 mmol) as the sulfur source. Reaction time: overnight for reaction 5, 2–3 hours for reaction 6. The reaction mixtures were subsequently neutralized with ammonia to adjust the pH to 4–5, frozen, and subjected to lyophilization overnight.

The resulting solid residues were extracted using a solid-liquid extraction with ethyl acetate followed by ethanol. After the solid-liquid extraction, each fraction (ethyl acetate-soluble, ethanol-soluble, and insoluble) was divided into two equal aliquots. One aliquot from each fraction was subjected to further purification via column chromatography, while the other was analyzed without additional purification. The NMR spectrum shown in **Figure 4.1** presents a comparison of the spectra for reactions 5 and 6.

^{1}H NMR (400 MHz, D_2O). δ (ppm) = 3.14 (s, 3H, 3a/5a), 3.26 (s, 9H, 3e-g/5e-g), 3.38 (m, 1H, 3c/5c), 3.60 (dd, 1H, 3c'/5c'), 3.90 (dd, 1H, 3d/5d), 7.22 (s, 1H, 5b), 8.40 (s, 1H, 3b).

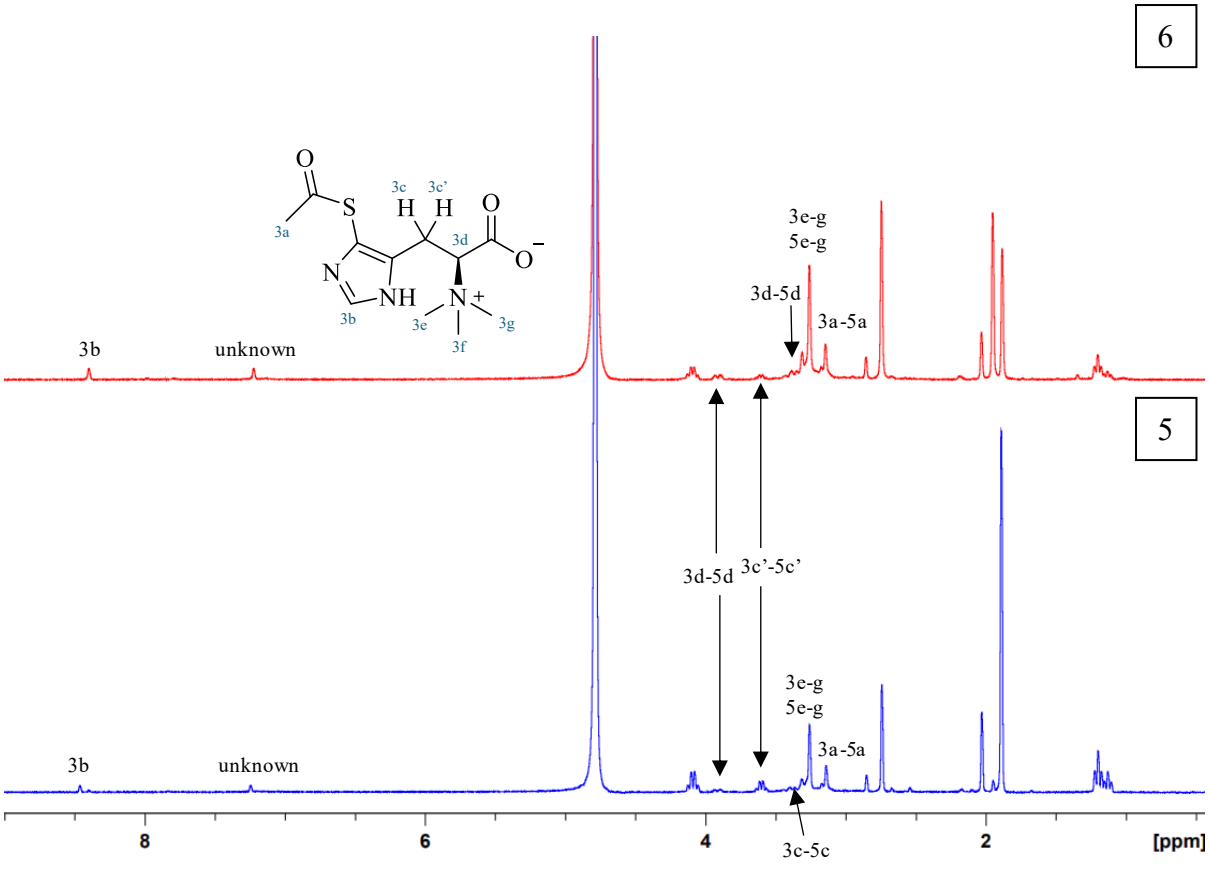

Figure 4.1. *Comparison of NMR spectra of reactions 5 and 6.*

General procedure C: reactions 7 to 10

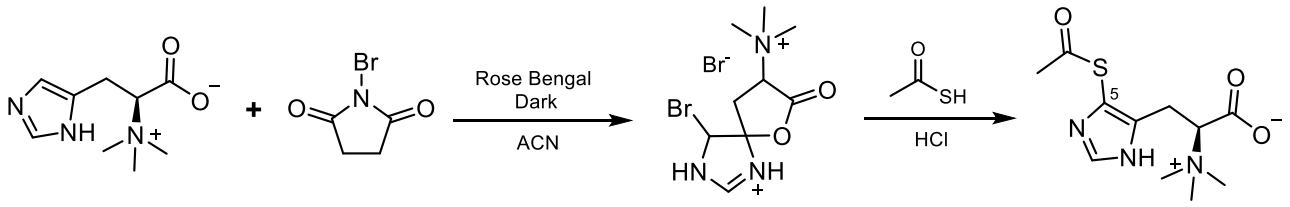

Reactions 7-9: *Synthesis of L-5-Acetylsulfanyl-α,N,N,N-trimethyl-histidine.*

For reactions 7 and 9, acetonitrile (2 mL, 1.572 g) was added to L-hercynine (98.62 mg, 0.50 mmol, 1 equiv.) in a reaction vial. The mixture was stirred vigorously for several minutes. NBS (97.90 mg, 0.55 mmol, 1.1 equiv.) and Rose Bengal (5.24 mg, 0.0050 mmol, 0.01 equiv.) were then introduced into the vial, and the reaction was conducted under dark conditions for one hour for reaction 7 and overnight for reaction 9. Following completion of the first step, acetonitrile was removed under reduced pressure using a rotary evaporator. The residue was dissolved in an aqueous HCl solution (164 µL of HCl in 2 mL of water), followed by the addition of thioacetic acid (400 µL, 5.5 mmol) as the sulfur source. The reaction was allowed to proceed overnight. Upon completion, the mixture was neutralized with ammonia to adjust the pH to 4–5, then frozen and subjected to lyophilization overnight to obtain the final product.

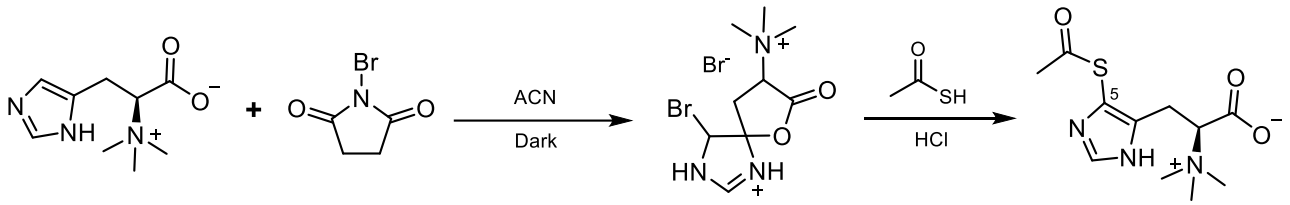

Reactions 8-10: *Synthesis of L-5-Acetylsulfanyl-α,N,N,N-trimethyl-histidine.*

For reactions 8 and 10, acetonitrile (2 mL, 1.572 g) was added to L-hercynine (98.62 mg, 0.50 mmol, 1 equiv.) in a reaction vial. The mixture was stirred vigorously for several minutes. NBS (97.90 mg, 0.55 mmol, 1.1 equiv.) was introduced into the vial, and the reaction was conducted under dark conditions for one hour for reaction 8 and overnight for reaction 10. Following completion of the first step, acetonitrile was removed under reduced pressure using a rotary evaporator.

The residue was dissolved in an aqueous HCl solution (164 µL of HCl in 2 mL of water), followed by the addition of thioacetic acid (400 µL, 5.5 mmol) as the sulfur source. The reaction was allowed to proceed overnight. Upon completion, the mixture was neutralized with ammonia to adjust the pH to 4–5, then frozen and subjected to lyophilization overnight to obtain the final product. Subsequent purification steps included solid-liquid extraction and column chromatography on a C18 reversed-phase column (elution solvent: water).

General procedure D: reactions 12 and 13

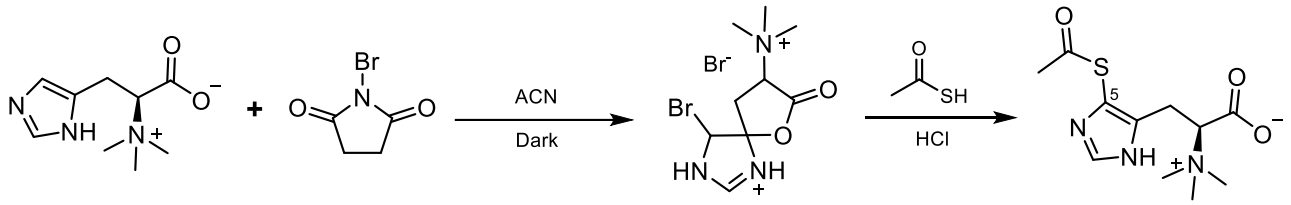

Reaction 12: *Synthesis of L-5-Acetylsulfanyl-α,N,N,N-trimethyl-histidine.*

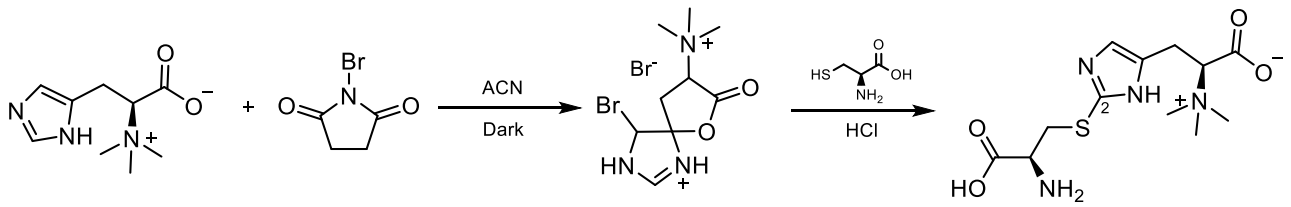

Reaction 13: *Synthesis of 3-{2-[(2-amino-2 carboxyethyl)thio]-1H-imidazol-4-yl}-2-(trimethylammonio) propanoate.*

Acetonitrile (20 mL, 15.72 g) was added to L-hercynine (0.986 g, 5 mmol, 1 equiv.) in a reaction flask. The mixture was stirred vigorously for several minutes. A notable observation during this step was the incomplete dissolution of hercynine in acetonitrile, necessitating a filtration step before the second reaction phase. The suspension was filtered to remove the insoluble fraction. For reaction 12, the recovered solid was weighed (0.2142 g), indicating that 0.7764 g (3.39 mmol) of hercynine had effectively dissolved and participated in the reaction. For reaction 13, the insoluble fraction was 0.3824, resulting in 0.6066 g (3.08 mmol) of dissolved hercynine used for the reaction.

NBS (0.979 g, 5.5 mmol, 1.1 equiv.) was then introduced into the vial, and the reaction was conducted under dark conditions overnight. Following completion of the first step, acetonitrile was removed under reduced pressure using a rotary evaporator. The residue was dissolved in an aqueous HCl solution (1.64 mL of HCl in 20 mL of water), followed by the addition of thioacetic acid (4 mL, 55 mmol) for reaction 12, and L-cysteine (0.606 g, 5 mmol) for reaction 13 as the sulfur source.

The reaction was allowed to proceed for 3 hours for reaction 12 and overnight for reaction 13. Upon completion, the mixture was neutralized with ammonia to adjust the pH to 4–5, then frozen and subjected to lyophilization overnight to obtain the final product. Subsequent purification steps included column chromatography on a C18 reversed-phase column (elution solvent: water).

Fractions containing the desired compound (identified by TLC) were collected and lyophilized, yielding 0.809 g of crude material for reaction 12. ^{1}H NMR analysis of the crude sample revealed a dominant presence of succinimide. Integration of a single aromatic proton signal from the desired product (~1H) against the succinimide region (~250H) indicated a product content of approximately 0.398%. Based on this estimate, the corrected mass of pure product was ~3.22 mg, corresponding to a ~0.30% yield relative to the amount of hercynine that had reacted.

Procedure for reaction 14

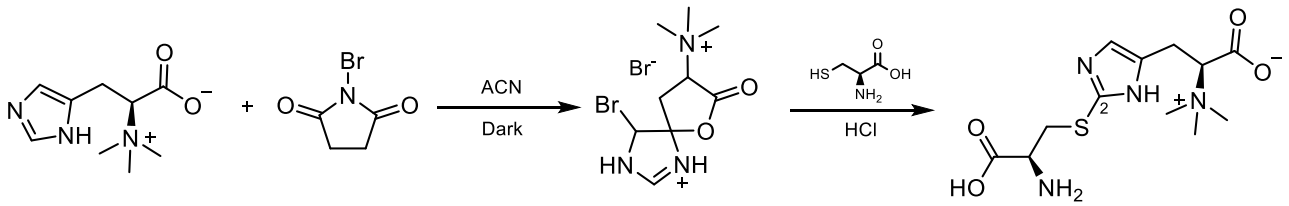

Reaction 14: *Synthesis of 3-{2-[(2-amino-2 carboxyethyl)thio]-1H-imidazol-4-yl}-2-(trimethylammonio) propanoate.*

Acetonitrile (40 mL) was added to L-hercynine (01.972 g, 10 mmol) in a reaction flask. The mixture was stirred vigorously for several minutes. NBS (1.958 g, 11 mmol) was introduced into the vial, and the reaction was conducted under dark conditions overnight.

Following completion of the first step, acetonitrile was removed under reduced pressure using a rotary evaporator. The residue was dissolved in an aqueous HCl solution (3.28 mL of HCl in 40 mL of water), followed by the addition of L-cysteine (1.212 g, 10 mmol) as the sulfur source. The reaction was allowed to proceed for 3 days.

Upon completion, the mixture was neutralized with ammonia to adjust the pH to 4–5, then frozen and subjected to lyophilization overnight to obtain the final product.

As a purification strategy, solid–liquid extraction was employed. To the dry reaction flask, ethyl acetate was first added, the solvent was filtered and the residue dried. This procedure was followed for isopropanol (which is more polar than ethyl acetate) and then ethanol. It was essential to quantify the amount of material dissolved in each solvent. Each extraction was monitored using thin-layer chromatography (TLC), with Gibbs reagent as a staining agent to aid visualization.

The NMR from solid-liquid extraction is shown in Chapter 2, "*Synthesis of Ergothioneine Derivative"*, **Figure 2.12**.

Incorporation of a liquid-liquid extraction step prior to solid-liquid extraction

5-acetylsulfanyl-histidine synthesis

Acetonitrile (30 mL) was added to L-hercynine (0.986 g, 5 mmol) in a reaction flask. The mixture was stirred vigorously for several minutes. A notable observation during this step was the incomplete dissolution of hercynine in acetonitrile, necessitating a filtration step before the second reaction phase.

The undissolved solids were removed by filtration and weighed (0.2445 g), resulting in 0.6620 g (3.36 mmol) of hercynine effectively used in the reaction. NBS (0.979 g, 5.5 mmol) was introduced into the vial, and the reaction was conducted under dark conditions overnight.

Following completion of the first step, acetonitrile was removed under reduced pressure using a rotary evaporator. The residue was dissolved in an aqueous HCl solution (1.64 mL of HCl in 20 mL of water), followed by the addition of thioacetic acid (4 mL, 55 mmol) as the sulfur source. The reaction was allowed to proceed for 3 hours.

Cysteinylhercynine synthesis

Acetonitrile (40 mL) was added to L-hercynine (1.479 g, 7.65 mmol) in a reaction flask. The mixture was stirred vigorously for several minutes. A notable observation during this step was the incomplete dissolution of hercynine in acetonitrile, necessitating a filtration step before the second reaction phase. The insoluble fraction (0.3870 g) was removed by filtration, leaving 1.0300 g (5.22 mmol) of dissolved hercynine. NBS (1.469 g, 8.20 mmol) was introduced into the vial, and the reaction was conducted under dark conditions overnight. Following completion of the first step, acetonitrile was removed under reduced pressure using a rotary evaporator. The residue was dissolved in an aqueous HCl solution (2.46 mL of HCl in 30 mL of water), followed by the addition of L-cysteine (1.818 g, 15 mmol) as the sulfur source. The reaction was allowed to proceed for 3 days.

General work up procedure:

Upon completion of the reaction, a liquid-liquid extraction with ethyl acetate was performed on reaction mixtures. The aqueous and organic phases were then separated, and each fraction was dried individually for both thiolated compounds. On the dried samples obtained from the aqueous phase, a solid-liquid extraction was carried out using ethyl acetate and isopropanol.

An important observation was made: the NMR spectrum of the ethyl acetate fraction derived from the liquid-liquid extraction of the thiolation reactions revealed a significant presence of succinimide, with the spectrum showing only the signal corresponding to this by-product at 2.9 ppm, as shown in **Figure 4.2**.

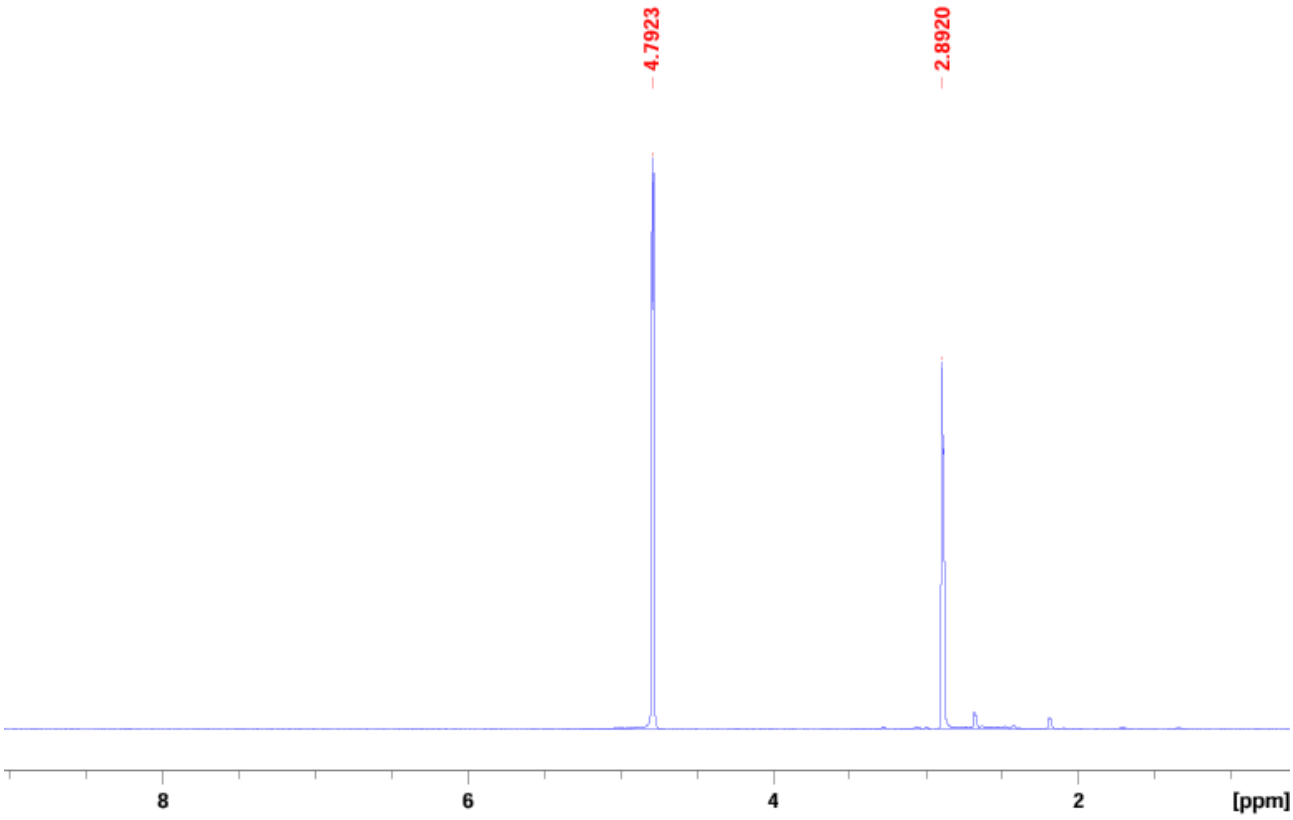

Figure 4.2. *NMR spectrum of the ethyl acetate fraction derived from the liquid-liquid extraction (organic phase).*

Also, solid–liquid extraction of the aqueous phase (previously freeze-dried) with isopropanol led to the removal of additional succinimide and NBS, without extracting the compound of interest, as shown in **Figure 4.3**.

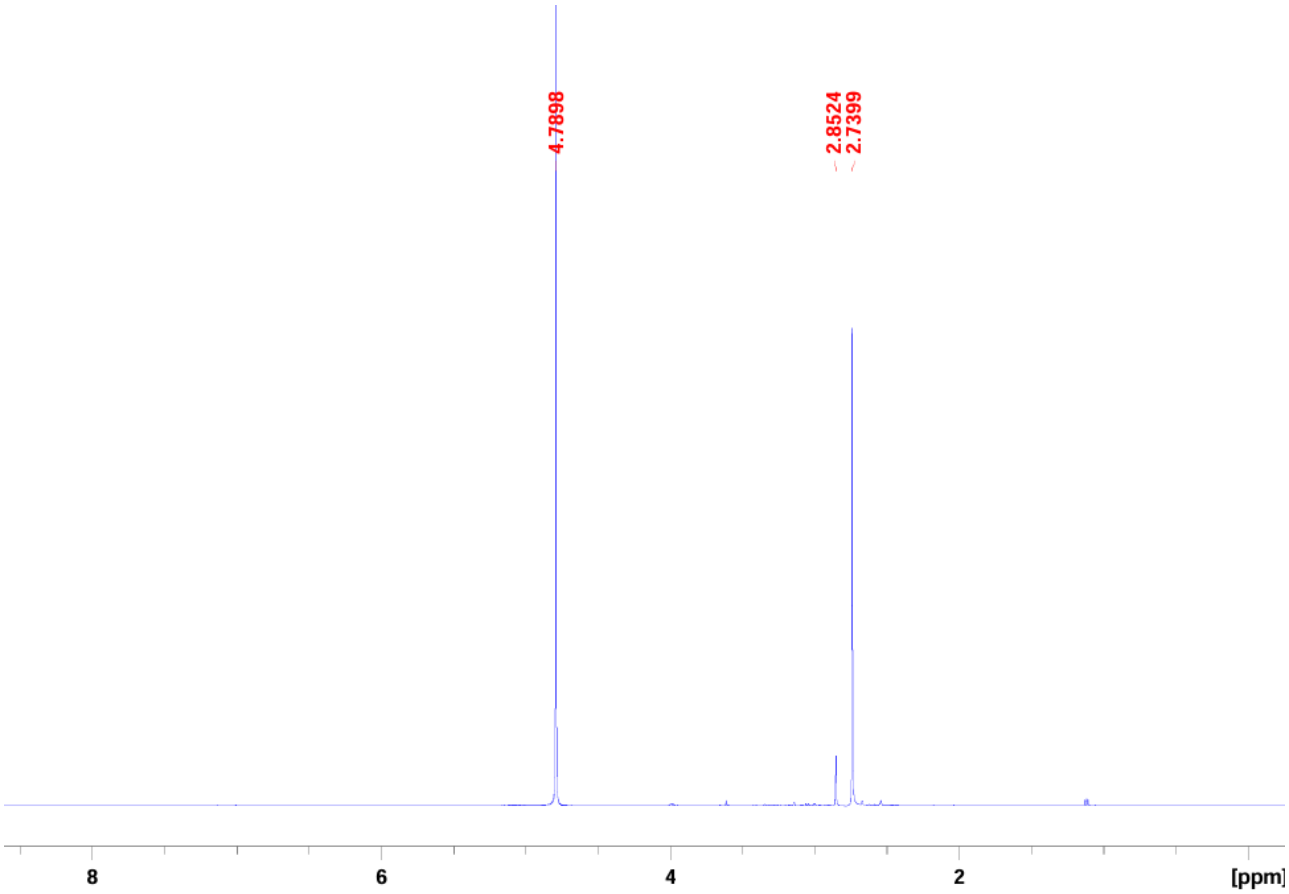

Figure 4.3. *NMR spectrum of the isopropanol fraction derived from the solid-liquid extraction (aqueous phase).*

With the solid-liquid extraction in ethyl acetate and isopropanol, succinimide was effectively separated, further reducing the presence of this by-product and improving the overall purity of the sample.

ABTS decolorization assay – TEAC assay

Preparation of buffers

Sodium acetate buffer pH 6.5: Sodium acetate (0.31 g) was dissolved in Milli-Q water (160 mL). Acetic acid (14.1 mg) was added to the solution. The mixture was then transferred to a 200 mL volumetric flask. The pH was adjusted to 6.5 using HCl and NaOH. The volume was made up to 200 mL using Milli-Q water.

PBS buffer pH 7.4: One PBS tablet was dissolved in water. The mixture was transferred to a 250 mL volumetric flask and the volume was made up using Milli-Q water.

TEAC assay

The antioxidant capacity of different thiols was measured. The samples analysed included L-(+)-ergothioneine, cysteine and penicillamine. Trolox, a vitamin E analogue, was used as a standard antioxidant for comparison.

The ABTS decolorization assay outlined in previously published studies was followed with some adjustments. A 7 mM ABTS stock solution was prepared by dissolving ABTS diammonium salt in sodium acetate buffer, pH 6.5.

A 245 mM sodium persulfate solution was prepared by dissolving sodium persulfate in sodium acetate buffer. Sodium persulfate solution was added to the ABTS stock solution so that the final concentration of the sodium persulfate solution was 2.45 mM. The mixture was incubated for 12-16 h at room temperature, while being protected from light. This generated the $ABTS^{\bullet+}$ radical cation which had a dark blue colour.

Table 4.1 provides a visual demonstration of the ABTS/$ABTS^{\bullet+}$ solutions at various stages throughout its preparation.

Table 4.1. Appearance of the ABTS/ABTS$^{\bullet+}$ solutions at various stages of preparation. A = ABTS in sodium acetate buffer pH 6.5; B = ABTS solution and sodium persulfate solution immediately upon mixing; C = ABTS$^{\bullet+}$ radical cation, 12-16 h after initial mixing.

A = ABTS (in sodium acetate buffer pH 6.5)	**B** = ABTS and sodium persulfate solution (immediately after mixing)	**C** = ABTS$^{\bullet+}$ radical cation (12-16 h after initial mixing)
		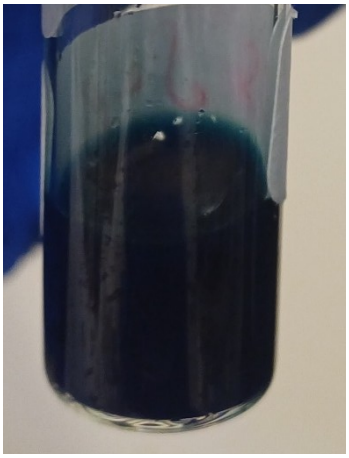

This radical was stable under these conditions for up to 60 h. The ABTS$^{\bullet+}$ radical cation is highly sensitive to light and must be protected from light when it is not being used.

Standard solutions ranging in concentration from 25-400 µM were prepared in quadruplicate for Trolox and 50-400 µM for each of the samples, using PBS buffer, pH 7.4.

The blank used to zero the UV-Vis spectrophotometer was a solution consisting of PBS buffer pH 7.4 (10 µL), sodium acetate buffer pH 6.5 (10 µL) and Milli-Q water (180 µL). The ABTS$^{\bullet+}$ stock solution was diluted with PBS to obtain an absorbance of 0.7 measured at 734 nm. (NB. The radical solution is highly sensitive to light and must be protected from light when it is not being used. The absorbance must be remeasured constantly and adjusted if needed. The absorbance decreases over-time).

Diluted $ABTS^{\bullet+}$ (1 mL) was added to each sample (50 μL), and the mixtures were equilibrated at 30 °C for 6 min. The absorbance of each sample was measured at 734 nm after 6 min of initial mixing. Each absorbance reading was measured in triplicate.

UV-Vis spectra of the $ABTS^{\bullet+}$ solution as well as each sample, at their different concentrations following the addition of $ABTS^{\bullet+}$ were measured at 500-900 nm.

The decolorization/inhibition (%) of each sample at the different concentrations was measured using the equation: $Decolorization\ (\%) = (\frac{Control\ Abs - Sample\ Abs}{Control\ Abs}) \times 100$, where the control abs is the absorbance of the $ABTS^{\bullet+}$ solution and the sample abs is the absorbance of the sample after the addition of $ABTS^{\bullet+}$ solution. Standard curves of each sample were generated showing inhibition (%) versus concentration (μM). The ratio between the gradient of the Trolox curve and each antioxidant curve was calculated to determine the TEAC value of each antioxidant.

General Conclusion and Future Work

The optimization of the synthesis and purification of ergothioneine derivatives represents a crucial step in the production of high-purity compounds for pharmaceutical and cosmetic applications. The results of this study highlight the importance of an integrated approach that considers not only reaction conditions but also targeted purification strategies to ensure the selectivity and integrity of the final product. The deprotection of the S-acetyl group was reported before an the efficiency of this final step toward L-5-sulfanyl-α-*N,N,N*-trimethyl-histidine was not repeated in this study. L-2-Acetylsulfanyl-α-*N,N,N*-trimethyl-histidine product (S-acetyl ergothioneine) was not detected under these reaction conditions. The purity of the L-5-acetylsulfanyl-α-*N,N,N*-trimethyl-histidine was determined by ^{1}H NMR and for the first time reported without the use of chromatography which is favorable for scale up.

Having access to synthetically produced L-5-acetylsulfanyl-α-*N,N,N*-trimethyl-histidine at an affordable cost would be extremely valuable, especially given the growing interest in antioxidants across the cosmetic, nutraceutical, and pharmaceutical industries. Natural sources like mushrooms often provide low yields and involve complex extraction procedures, which limit scalability. Developing a reliable and scalable synthetic route could guarantee consistent quality and availability, making it easier to incorporate ergothioneine and its regioisomer into a wide range of consumer products. This aligns closely with the main goal of this work, which is to establish an efficient and practical approach, both synthetic and analytical, for studying and applying ergothioneine-based antioxidants.

One of the key aspects that emerged is the balance between reaction efficiency and selectivity, which required progressive refinement of the experimental conditions.

The strategic use of solvents, particularly the employment of acetonitrile in the initial phase followed by aqueous HCl in the subsequent step, proved effective in enhancing reagent solubility without compromising the stability of the final product. This approach minimized exposure to strong acids, improving the sustainability of the process while reducing the risk of thermal or chemical degradation.

In parallel, the refinement of purification techniques played a decisive role in achieving high purity standards. The limitations of chromatography, particularly the co-elution of structurally similar impurities, necessitated the implementation of alternative strategies such as solid-liquid extractions with a gradient of solvent polarities. The sequential use of ethyl acetate, isopropanol, and ethanol enabled the efficient separation of the desired product from reaction by-products, while the subsequent freeze-drying process ensured the complete removal of residual solvents.

From a theoretical perspective, these findings reaffirm the crucial role of solvent properties in organic synthesis. The dielectric constant and a solvent's ability to stabilize ionic or polar species were key factors in guiding the choice of reaction and purification media. This demonstrates how a careful modulation of solvent-solute interactions can significantly impact the efficiency of synthetic processes.

Despite the progress achieved, there are still areas for improvement that future studies could explore. One particularly promising avenue involves optimizing reaction conditions to further increase yields and reduce by-product formation. Additionally, integrating purification methods based on advanced technologies could offer significant advantages in terms of separation efficiency and the reduction of organic solvent consumption. These approaches not only contribute to a more sustainable process but also enhance resolution in the removal of structurally similar impurities. For instance, the use of greener solvents helps reduce environmental impact compared to traditional solvents. This can improve the sustainability and cost-efficiency of the overall process.

Prioritizing low-toxicity, biodegradable solvents and implementing solvent recovery systems are essential steps toward greener chemistry and alignment with current environmental regulations.

Another valuable area for exploration involves the characterization of synthesized products using advanced spectroscopic techniques, such as two-dimensional nuclear magnetic resonance (2D-NMR) and high-resolution mass spectrometry (HRMS). These analytical tools could provide more detailed insights into the structure of synthesized derivatives, leading to a deeper understanding of their physicochemical properties and long-term stability.

Moreover, further purification methods should be investigated to efficiently remove residual succinimide, NBS, and solvent traces from the final product mixture. Ion exchange chromatography, for instance, could be an effective approach to separate these components. However, a compromise in scale up cost would be inevitable. Scale up procedures would potentialy involve a spray drying step for the final product.

Upon obtaining a highly pure compound, its antioxidant properties can be systematically evaluated using the ABTS decolorization assay, a well-established method that offers an accurate means of comparing the radical scavenging activity of the synthesized compound against reference antioxidants such as Trolox and L-(+)-ergothioneine. This step is fundamental, as it will provide a deeper understanding of the compound's potential as an effective antioxidant in biological and pharmaceutical contexts. By comparing its antioxidant activity with that of well-established standards, such as Trolox, a synthetic vitamin E analogue, and L-(+)-ergothioneine, a naturally occurring thiol, we can assess the compound's efficiency in neutralizing free radicals, and its potential relevance in mitigating oxidative stress within living systems.

The ability to evaluate compounds using the ABTS assay also opens doors to their application in various biomedical and pharmaceutical fields.

Antioxidants play a crucial role in the prevention of oxidative stress-related diseases, such as neurodegenerative disorders, cardiovascular diseases, and inflammatory conditions. Therefore, assessing the antioxidant properties of ergothioneine derivatives will provide valuable insights into their therapeutic potential.

Given that ergothioneine is known for its unique biological activity, particularly in protecting tissues from oxidative damage, any derivatives with improved or enhanced properties could have significant implications for both human health and disease prevention. This work has successfully established a reliable protocol for the synthesis and purification of ergothioneine derivatives, which forms a solid foundation for future research in this area.

Due to technical issues encountered with the UPLC-MS/MS instrument during this project, the planned method development for the quantification of L-(+)-ergothioneine was not completed during this period. This aspect of the research were initiated however, the results will be considered as part of future studies.

Once established, this method will allow for the analysis of L-(+)-ergothioneine levels in various cosmetic formulations, such as face creams, to evaluate its presence and potential efficacy as an antioxidant ingredient. Additionally, the method will be employed to assess the ergothioneine content in different edible mushrooms, including portabellini, exotic oyster mushrooms, shimeji, and king oyster mushrooms, as well as in commercially available mushroom extracts, like Reishi. This work will provide essential insights into the natural dietary sources of ergothioneine, highlighting its potential applications in functional foods, nutraceuticals, and skincare products.

In conclusion, this study represents a significant step forward in the synthesis, purification, and analysis of ergothioneine derivatives, laying the groundwork for further exploration of their antioxidant properties. The findings contribute to the broader understanding of ergothioneine's potential as a biologically relevant antioxidant.

As research continues, the insights gained will drive future work toward the development of novel antioxidant compounds with promising applications in health, pharmaceuticals, and beyond.

References

1. Tanret C. Sur une base nouvelle retiree du seigle ergote, l'ergothioneine. *Compt Rend*. 149:222-224.

2. Aruoma OI, Spencer JP, Mahmood N. Protection against oxidative damage and cell death by the natural antioxidant ergothioneine. *Food Chem Toxicol*. 1999;37(11):1043-1053. doi:10.1016/s0278-6915(99)00098-8

3. Sao Emani C, Gallant JL, Wiid IJ, Baker B. The role of low molecular weight thiols in Mycobacterium tuberculosis. *Tuberculosis (Edinb)*. 2019;116:44-55. doi:10.1016/j.tube.2019.04.003

4. Tang RMY, Cheah IKM, Yew TSK, Halliwell B. Distribution and accumulation of dietary ergothioneine and its metabolites in mouse tissues. *Sci Rep*. 2018;8(1):1601. doi:10.1038/s41598-018-20021-z

5. Dubost NJ, Ou B, Beelman RB. Quantification of polyphenols and ergothioneine in cultivated mushrooms and correlation to total antioxidant capacity. *Food Chemistry*. 2007;105(2):727-735. doi:10.1016/j.foodchem.2007.01.030

6. Wardman P, von Sonntag C. Kinetic factors that control the fate of thiyl radicals in cells. *Methods Enzymol*. 1995;251:31-45. doi:10.1016/0076-6879(95)51108-3

7. Yardim-Akaydin S, Sepici A, Ozkan Y, Simşek B, Sepici V. Evaluation of allantoin levels as a new marker of oxidative stress in Behçet's disease. *Scand J Rheumatol*. 2006;35(1):61-64. doi:10.1080/03009740510026878

8. Fu TT, Shen L. Ergothioneine as a Natural Antioxidant Against Oxidative Stress-Related Diseases. *Front Pharmacol*. 2022;13:850813. doi:10.3389/fphar.2022.850813

9. Kalaras MD, Richie JP, Calcagnotto A, Beelman RB. Mushrooms: A rich source of the antioxidants ergothioneine and glutathione. *Food Chem*. 2017;233:429-433. doi:10.1016/j.foodchem.2017.04.109

10. Tsiantas K, Tsiaka T, Koutrotsios G, et al. On the Identification and Quantification of Ergothioneine and Lovastatin in Various Mushroom Species: Assets and Challenges of Different Analytical Approaches. *Molecules*. 2021;26(7):1832. doi:10.3390/molecules26071832

11. EFSA Panel on Dietetic Products, Nutrition and Allergies (NDA), Turck D, Bresson JL, et al. Statement on the safety of synthetic l-ergothioneine as a novel food - supplementary dietary exposure and safety assessment for infants and young children, pregnant and breastfeeding women. *EFSA J*. 2017;15(11):e05060. doi:10.2903/j.efsa.2017.5060

12. Erdelmeier I, Daunay S, Lebel R, Farescour L, Yadan JC. Cysteine as a sustainable sulfur reagent for the protecting-group-free synthesis of sulfur-containing amino acids: biomimetic synthesis of l-ergothioneine in water. *Green Chem*. 2012;14(8):2256. doi:10.1039/c2gc35367a

13. Halliwell B, Cheah IK, Tang RMY. Ergothioneine – a diet-derived antioxidant with therapeutic potential. *FEBS Letters*. 2018;592(20):3357.

14. Ey J, Schömig E, Taubert D. Dietary Sources and Antioxidant Effects of Ergothioneine. *J Agric Food Chem*. 2007;55(16):6466-6474. doi:10.1021/jf071328f

15. Wijesekara T, Xu B. Occurrence, dietary sources, quantification and bioactivities of natural antioxidant ergothioneine – A longavity vitamin? *International Journal of Food Science & Technology*. 2024;59(9):5951-5963. doi:10.1111/ijfs.17414

16. Gao W, Wang Y, Wang F, Wu X, Lu F, Liu F. Ergothioneine exerts neuroprotective effects in Parkinson's disease: Targeting α-synuclein aggregation and oxidative stress. *Food Research International*. 2025;201:115590. doi:10.1016/j.foodres.2024.115590

17. Sakata S, Kunimatsu R, Tanimoto K. Protective Effect of Ergothioneine against Oxidative Stress-Induced Chondrocyte Death. *Antioxidants (Basel)*. 2024;13(7):800. doi:10.3390/antiox13070800

18. Libby P, Ridker PM, Hansson GK. Progress and challenges in translating the biology of atherosclerosis. *Nature*. 2011;473(7347):317-325. doi:10.1038/nature10146

19. Hussain T, Tan B, Yin Y, Blachier F, Tossou MCB, Rahu N. Oxidative Stress and Inflammation: What Polyphenols Can Do for Us? *Oxid Med Cell Longev*. 2016;2016:7432797. doi:10.1155/2016/7432797

20. Chen L, Zhang L, Ye X, Deng Z, Zhao C. Ergothioneine and its congeners: anti-ageing mechanisms and pharmacophore biosynthesis. *Protein Cell*. 2024;15(3):191-206. doi:10.1093/procel/pwad048

21. Han Y, Tang X, Zhang Y, Hu X, Ren LJ. The current status of biotechnological production and the application of a novel antioxidant ergothioneine. *Crit Rev Biotechnol*. 2021;41(4):580-593. doi:10.1080/07388551.2020.1869692

22. Markova NG, Karaman-Jurukovska N, Dong KK, Damaghi N, Smiles KA, Yarosh DB. Skin cells and tissue are capable of using l-ergothioneine as an integral component of their antioxidant defense system. *Free Radical Biology and Medicine*. 2009;46(8):1168-1176. doi:10.1016/j.freeradbiomed.2009.01.021

23. Anti-Aging Claim Support Testing Lab - Validated Claim Support. Accessed March 18, 2025. https://validatedcs.com/consumer-product-testing/anti-aging-claims/

24. Khonde PL, Jardine A. Improved synthesis of the super antioxidant, ergothioneine, and its biosynthetic pathway intermediates. *Org Biomol Chem*. 2015;13(5):1415-1419. doi:10.1039/c4ob02023e

25. Wei L, Liu L, Gong W. Structure of mycobacterial ergothioneine-biosynthesis C-S lyase EgtE. *Journal of Biological Chemistry*. 2024;300(1). doi:10.1016/j.jbc.2023.105539

26. al SS et. Biosynthesis of ergothioneine: current state, achievements, and perspectives | EndNote Click. Accessed June 15, 2025. https://click.endnote.com/viewer?doi=10.1007%2Fs00253-025-13476-4&token=WzQ0MzYxNDQsIjEwLjEwMDcvczAwMjUzLTAyNS0xMzQ3Ni00Il0.0hrcipMKpwSOyWbm_DWM5dgGedM

27. Brosnan JT, Brosnan ME. The Sulfur-Containing Amino Acids: An Overview12. *The Journal of Nutrition*. 2006;136(6):1636S-1640S. doi:10.1093/jn/136.6.1636S

28. Paulsen CE, Carroll KS. Cysteine-mediated redox signaling: chemistry, biology, and tools for discovery. *Chem Rev*. 2013;113(7):4633-4679. doi:10.1021/cr300163e

29. Seebeck FP. In Vitro Reconstitution of Mycobacterial Ergothioneine Biosynthesis. *J Am Chem Soc*. 2010;132(19):6632-6633. doi:10.1021/ja101721e

30. Xu J, Yadan JC. Synthesis of L-(+)-Ergothioneine. *J Org Chem*. 1995;60(20):6296-6301. doi:10.1021/jo00125a014

31. Klijn JE, Engberts JBFN. Fast reactions 'on water.' *Nature*. 2005;435(7043):746-747. doi:10.1038/435746a

32. Daunay S, Lebel R, Farescour L, Yadan JC, Erdelmeier I. Short protecting-group-free synthesis of 5-acetylsulfanyl-histidines in water: novel precursors of 5-sulfanyl-histidine and its analogues. *Org Biomol Chem*. 2016;14(44):10473-10480. doi:10.1039/C6OB01870J

33. Hornbrook LF, Reed CD, Lamar AA. Bromination of indazoles enhanced by organic-dye, visible-light photoredox catalysis. *Tetrahedron*. 2023;142:133523. doi:10.1016/j.tet.2023.133523

34. Saada MC, Vullo D, Montero JL, Scozzafava A, Supuran CT, Winum JY. Mono- and di-halogenated histamine, histidine and carnosine derivatives are potent carbonic anhydrase I, II, VII, XII and XIV activators. *Bioorganic & Medicinal Chemistry*. 2014;22(17):4752-4758. doi:10.1016/j.bmc.2014.07.005

35. Jain R, Avramovitch B, Cohen LA. Synthesis of ring-halogenated histidines and histamines. *Tetrahedron*. 1998;54(13):3235-3242. doi:10.1016/S0040-4020(98)00068-4

36. Cerezo V, Afonso A, Planas M, Feliu L. Synthesis of 5-arylhistidines via a Suzuki–Miyaura cross-coupling. *Tetrahedron*. 2007;63(42):10445-10453. doi:10.1016/j.tet.2007.08.010

37. Evanno FE and ED and L. User-friendly and Green Procedure for a Photoinduced Wohl-Ziegler Reaction | EndNote Click. Accessed June 15, 2025.

https://click.endnote.com/viewer?doi=10.1002%2Fejoc.202500183&token=WzQ0MzYxNDQsIjEwLjEwMDIvZWpvYy4yMDI1MDAxODMiXQ.iRKuxXSFXfDqKffF1El2iOidvMw

38. Sotgia S, Mangoni A, Forteschi M, et al. Identification of the Main Intermediate Precursor of l-Ergothioneine Biosynthesis in Human Biological Specimens. *Molecules*. 2016;21(10):1298. doi:10.3390/molecules21101298

39. Josephy PDavid, Van Damme Anjel. Reaction of Gibbs reagent with para-substituted phenols. *Anal Chem*. 1984;56(4):813-814. doi:10.1021/ac00268a052

40. Cano A, Maestre AB, Hernández-Ruiz J, Arnao MB. ABTS/TAC Methodology: Main Milestones and Recent Applications. *Processes*. 2023;11(1):185. doi:10.3390/pr11010185

41. Munteanu IG, Apetrei C. Analytical Methods Used in Determining Antioxidant Activity: A Review. *Int J Mol Sci*. 2021;22(7):3380. doi:10.3390/ijms22073380

42. Apak R, Güçlü K, Demirata B, et al. Comparative evaluation of various total antioxidant capacity assays applied to phenolic compounds with the CUPRAC assay. *Molecules*. 2007;12(7):1496-1547. doi:10.3390/12071496

43. Kut K, Cieniek B, Stefaniuk I, Bartosz G, Sadowska-Bartosz I. A Modification of the ABTS• Decolorization Method and an Insight into Its Mechanism. *Processes*. 2022;10(7):1288. doi:10.3390/pr10071288

44. Sadowska-Bartosz I, Bartosz G. Evaluation of The Antioxidant Capacity of Food Products: Methods, Applications and Limitations. *Processes*. 2022;10(10):2031. doi:10.3390/pr10102031

45. Miller NJ, Rice-Evans C, Davies MJ, Gopinathan V, Milner A. A novel method for measuring antioxidant capacity and its application to monitoring the antioxidant status in premature neonates. *Clin Sci (Lond)*. 1993;84(4):407-412. doi:10.1042/cs0840407

46. Re R, Pellegrini N, Proteggente A, Pannala A, Yang M, Rice-Evans C. Antioxidant activity applying an improved ABTS radical cation decolorization assay. *Free Radic Biol Med*. 1999;26(9-10):1231-1237. doi:10.1016/s0891-5849(98)00315-3

47. Ilyasov IR, Beloborodov VL, Selivanova IA, Terekhov RP. ABTS/PP Decolorization Assay of Antioxidant Capacity Reaction Pathways. *Int J Mol Sci*. 2020;21(3):1131. doi:10.3390/ijms21031131

48. Pisoschi A, Negulescu G. Methods for Total Antioxidant Activity Determination: A Review. *Biochemistry & Analytical Biochemistry*. 2012;01. doi:10.4172/2161-1009.1000106

49. Schaich KM, Tian X, Xie J. Hurdles and pitfalls in measuring antioxidant efficacy: A critical evaluation of ABTS, DPPH, and ORAC assays. *Journal of Functional Foods*. 2015;14:111-125. doi:10.1016/j.jff.2015.01.043

50. Moreira D. *ABTS Decolorization Assay – in Vitro Antioxidant Capacity V1*.; 2019. doi:10.17504/protocols.io.42xgyfn

51. Sotgia S, Taras A, Zinellu A, et al. Hercynine, Ergothioneine and Redox State in Stallion's Seminal Plasma. *Antioxidants (Basel)*. 2020;9(9):855. doi:10.3390/antiox9090855

52. Franzoni F, Colognato R, Galetta F, et al. An in vitro study on the free radical scavenging capacity of ergothioneine: comparison with reduced glutathione, uric acid and trolox. *Biomed Pharmacother*. 2006;60(8):453-457. doi:10.1016/j.biopha.2006.07.015

53. Liu L, Sun L, Fan S, et al. Determination of L-Ergothioneine in Cosmetics Based on Ultraperformance Liquid Chromatography-Tandem Mass Spectrometry. *International Journal of Analytical Chemistry*. 2022;2022(1):4372295. doi:10.1155/2022/4372295

54. Hrabárová E, Valachová K, Rapta P, Šoltés L. An Alternative Standard for Trolox-Equivalent Antioxidant-Capacity Estimation Based on Thiol Antioxidants. Comparative 2,2′-Azinobis[3-ethylbenzothiazoline-6-sulfonic Acid] Decolorization and Rotational Viscometry Study Regarding Hyaluronan Degradation. *Chemistry & Biodiversity*. 2010;7(9):2191-2200. doi:10.1002/cbdv.201000019